(Preprint) AAS 25-099

GENERALIZED REFERENCE TARGETING FOR SPACEFLIGHT

David Geller[*], David Woffinden[†], Collin York[‡]

For spaceflight programs to achieve some of the aggressive exploration initiatives such as visiting and landing on other celestial bodies, rendezvousing with other orbiting vehicles, and ultimately returning crew safely to Earth, an assortment of targeting algorithms to compute the necessary burns to strategically maneuver a spacecraft to a variety of destinations are required. Numerous examples exist, but rather than creating and implementing multiple targeting solutions, is it possible to have a general targeting model that can accommodate a variety of applications? Originally motivated for mission design and analysis purposes, this paper outlines a generalized reference targeting algorithm for spaceflight that may also have applications in on-orbit flight software. It accommodates arbitrary flight dynamics and both impulsive and finite burns for either absolute or relative targeting applications. It also allows for an arbitrary number of targeting design parameters such as multiple discrete correction burns or finite thrust parameters to satisfy numerous combinations of targeting constraints that can have fixed or variable time epochs. Given a reference trajectory, this targeting technique provides a general framework to quickly solve an assortment of targeting problems that may be well-defined, over-determined, or under-determined while naturally producing metrics providing insight into the controllability for a given problem formulation. Due to the derivation, speed, and accuracy of the algorithm, it lends to supporting rapid linear covariance analysis and robust trajectory design applications for a variety of flight phases such as rendezvous and docking, cislunar transfer, interplanetary flight, orbit maintenance, de-orbit, and powered descent and landing.

1 INTRODUCTION

As space exploration continues to advance and the possible missions and destinations expand, an increased capability in the scope and breadth of targeting algorithms continues to emerge. Past and current programs have demanded and produced an assortment of targeting algorithms to address rendezvous and docking needs, deep space exploration initiatives, and classical orbital transfer scenarios. These algorithms such as the classic Lambert targeting for orbit transfers or the well utilized and linear Clohessy Wiltshire (CW) targeting for rendezvous, and the more recently developed and complex two-level targeter (TLT) for the Orion spacecraft utilized for deep space exploration reflect the wide-assortment of targeting problems being addressed. Rather than creating and implementing multiple targeting solutions to enable spaceflight programs to achieve some of the aggressive exploration initiatives, is it possible to have a general targeting model that can accommodate a variety of applications? Originally motivated for mission design and analysis purposes, this paper outlines a generalized reference targeting algorithm for spaceflight that may also have applications in on-orbit flight software.

The literature is replete with nonlinear targeting algorithms based on shooting methods and other means to solve complex nonlinear problems.[1, 2, 3, 4, 5, 6]. In many cases the solution approach is designed specifically for (or reused from) a particular application. Embedded in these solutions is often a correction process based on the linearized equations of motion, and the theory of these linear equations and there numerical applications is well known [7, 8].

[*]Distinguished Engineer/Scientist, Strategic Military Space Division, Utah State University Space Dynamics Laboratory, 416 East Innovation Avenue, North Logan, UT 84341

[†]Aerospace Engineer, GN&C Autonomous Flight Systems Branch, NASA Johnson Space Center, Houston Tx, 77058

[‡]Aerospace Engineer, GN&C Autonomous Flight Systems Branch, NASA Johnson Space Center, Houston Tx, 77058

With this context, the purpose of this paper is to present a unified approach to linear targeting problems for spaceflight applications. If such a paper already exists, it is unknown to the authors. The underlying linear theory in this paper is not new; however, a single generalized formulation for solving arbitrary spaceflight targeting problems is developed. It accommodates arbitrary flight dynamics and both impulsive and finite burns for either absolute or relative targeting applications. It also allows for an arbitrary number of targeting design parameters such as multiple discrete correction burns or finite thrust parameters to satisfy numerous combinations of targeting constraints that can have fixed or variable time epochs.

Given a reference trajectory, this targeting technique provides a general framework to quickly solve an assortment of targeting problems that may be well-determined, over-determined, or under-determined while naturally producing metrics providing insight into the controllability for a given problem formulation. Due to the derivation, speed, and accuracy of the algorithm, it lends to supporting rapid linear covariance analysis and robust trajectory design applications for a variety of flight phases such as rendezvous and docking, cislunar transfer, interplanetary flight, orbit maintenance, de-orbit, and powered descent and landing.

The development of the generalized reference targeting (GRT) algorithm is initiated by first providing a basic overview comparing different targeting methods for analysis followed by outlining the common GRT framework to solve both well-defined, over-determined, and under-determined problems that manifests itself for a spectrum of problems in Section 2 and Section 3 respectively. Given this modular problem formulation, details for capturing the generalized formulation for arbitrary targeting parameters and constraints are presented in context of impulsive translational burns in Section 4, finite burn targeting in Sections 5 and 6, and relative targeting in Section 7. The theoretical development is then applied to a lunar orbital escape problem in Section 8 with three examples using GRT with either impulsive or finite burns. The first example uses GRT with impulsive maneuvers and variable constraint times. The second then utilizes GRT with finite burns with variable thrust vector, ignition time, variable engine cutoff time, and variable constraint times. The last example uses finite burns with a fixed thrust magnitude and allowing the thrust direction and turn rate to vary. These examples illustrate the core capability and flexibility of the algorithm while also highlighting the impact of calculating the targeted burn at different intervals prior to the burn execution. Final remarks and conclusions are then provided Section 9.

2 TARGETING METHODS COMPARISON OVERVIEW

Prior to deriving the generalized reference targeting or GRT algorithms for impulsive and finite burns, a simplified comparison overview of targeting methods for spaceflight analysis is provided to give context to the limitations and potential of GRT. Figure 1 highlights three-levels of targeting fidelity with the simplicity and speed toward the right and complexity and flexibility on the left.

Figure 1(a) captures a general non-linear targeting algorithm that only requires a *reasonable* initial guess and the solution is computed iteratively. It does not require an a priori reference trajectory. The state relationship matrices (SRM) and constraint partials are modified with each iteration. These types of non-linear predictor algorithms may also compute the targeting partials numerically at each iteration via finite difference, handles equality and inequality constraints, and provide maneuver partials with flexibility for changing constraints and initial guesses. This generality and capability to address a wide range of problems with limited a priori information comes at the price of longer run times.

Figure 1(b) emphasizes how GRT can be expanded by adopting an iterative non-linear predictor. Although the pre-generated SRMs and constraint partials are derived based on the a priori reference trajectory, the linear correction solution is iterated by using a non-linear trajectory propagator to determine if the constraint tolerance was satisfied. If not, the correction is modified using the pre-generated partials until an iterative solution converges. This approach assumes the reference trajectory provided represents a viable solution, so if the dispersions are within the linear regime of the reference profile, few iterations should be required.

Figure 1(c) captures the basic *linear* implementation of GRT intended for rapid analysis. If the system dynamics are truly (or assumed to be) linear such as the CW-equations [9] for the relative motion dynamics near a target vehicle in a circular orbit near a central body, GRT can be configured to produce the well-known CW-targeting equations. For applications with non-linear dynamics, GRT requires an a priori non-

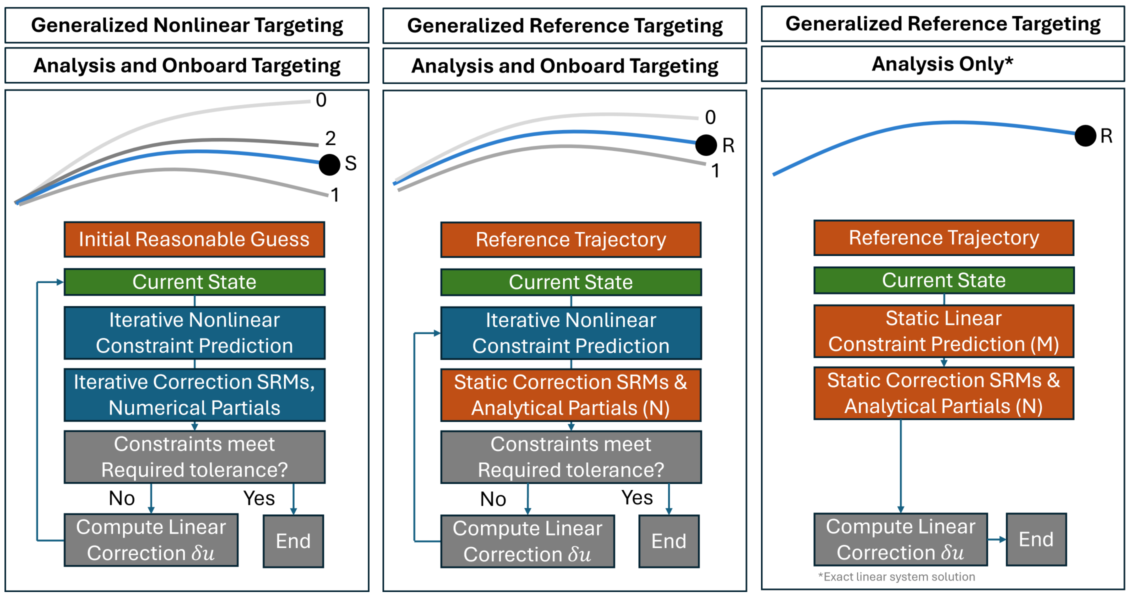

(a) Generalized Nonlinear Targeting (b) Nonlinear GRT (c) Linear GRT

Figure 1. Comparison of Targeting Methods for Analysis

linear reference profile which serves as the targeting solution. The targeting state transition matrix (STM) and constraint partials are computed exactly along the reference trajectory using a semi-analytic evaluation. Consequently, it provides a rapid evaluation of maneuver partials when a solution and analytic expressions are provided.

3 GENERALIZED REFERENCE TARGETING FRAMEWORK

If a reference trajectory is provided $x^*(t)$, then the objective of the generalized reference targeting algorithm is to determine the dispersion from the nominal burn parameters δu required to achieve the targeting constraints. The myriad of targeting problems can all be cast as a set of m linear equations of the following common and general form

$$\boxed{\mathcal{M}\delta u = \mathcal{N}\delta x(t_0^*)} \tag{1}$$

where δu represents n parameters to be solved for, and $\delta x(t_0^*)$ represents the initial position and velocity dispersion from the reference trajectory. For finite burns, $\delta x(t_0^*)$ will also include the initial mass dispersion and initial thrust Isp dispersion.

For the impulsive targeting implementation the n targeting parameters are single or multiple impulsive Δv maneuvers and variable constraint times. For the finite-burn targeting algorithm, the n parameters are the engine ignition time, a perturbation to the thrust vector or the direction and rotation rate of the thrust vector, the thrust cutoff time, and an optional variable constraint time.

When the number of targeting design parameters equals the number of linear equations, $m = n$, Eq 1 represents a well-defined problem whose solution for the targeting design parameters δu is obtained simply by taking the inverse of $\mathcal{M}^{-1}$

$$\delta u = \mathcal{M}^{-1}\mathcal{N}\delta x(t_0^*) \tag{2}$$

When the number of linear equations is greater than the number of control inputs, $m > n$, Eq 1 represents an over-determined problem and a solution for the minimum constraint error norm is desired

$$\delta u = (\mathcal{M}^T W_\psi \mathcal{M})^{-1}\mathcal{M}^T W_\psi \mathcal{N}\delta x(t_0^*) \tag{3}$$

where the constraints may be weighted by a diagonal matrix W_ψ. When the number of linear equations is less than the number of targeting control parameters, $m < n$, Eq 1 represents an under-determined problem and a solution to the minimum parameter norm is desired

$$\delta u = W_c \mathcal{M}^T (\mathcal{M} W_c \mathcal{M}^T)^{-1} \mathcal{N} \delta x(t_0^*) \tag{4}$$

Regardless on how the targeting problem is formulated, ($m = n$, $m > n$, or $m < n$), one of the above three solutions to Eq 1 will be available. The next four major sections demonstrate how this generalized reference targeting framework is implemented to solve the targeting problems associated with impulsive or discrete burns, finite-thrust burns, and the dual inertial relative state targeting problems.

4 GRT USING IMPULSIVE BURNS

When the position and velocity dispersion from a desired reference trajectory are zero, all trajectory constraints will by definition be satisfied. However, when the position and velocity dispersion are non-zero, a single or multiple corrective impulsive maneuvers may be needed to meet mission requirements. For many applications, modeling the translational burn as an instantaneous velocity change or impulsive Δv is adequate. This section will highlight several targeting options that are derived and presented in context of impulsive-burn targeting. The three potential options are: 1) one impulsive burn and one set of constraints at a single time, 2) one impulsive burn and multiple sets of constraints at multiple times, and 3) multiple impulsive burns and multiple sets of constraints at multiple times. The objective of these targeting algorithms is to correct nominal maneuver parameters based on initial trajectory dispersion to ensure trajectory constraints are satisfied.

Underlying the derivations that follow in this section is the assumption that a reference trajectory satisfying all trajectory constraints is available. The reference trajectory may include nominal impulsive maneuvers. The nonlinear coasting-flight dynamics in between the nominal impulsive maneuvers for a vehicle with inertial position $r(t)$ and velocity $v(t)$ are most generally given by

$$\dot{x} = f(x)$$

where the state x represents the vehicle position and velocity $x = [r, v]^T$. For inertial dynamics with an arbitrary gravity field

$$\dot{r} = v \tag{5}$$
$$\dot{v} = g(r) \tag{6}$$

the associated linearized differential equations of motion are given by

$$\delta \dot{x} = F \delta x, \quad F = \begin{bmatrix} 0 & I \\ G & 0 \end{bmatrix} \tag{7}$$

where $\delta x = [\delta r, \delta v]^T$ defines the coasting-flight state dispersion from the reference trajectory, i.e., $\delta r = r - r^*$, $\delta v = v - v^*(t)$, and where G is given by

$$G = \left. \frac{\partial g(r)}{\partial r} \right|_* \tag{8}$$

For non-inertial dynamics such as the CW-equations [9] or the restricted 3-body problem (R3BP) in a rotating frame [10], the Jacobian F in Eq. 7 is simply replaced with the appropriate Jacobian, $F = F_{CW}$ or $F = F_{R3BP}$. Thus, for arbitrary dynamics, the discrete-time format for the state dispersion at time t is given by

$$\delta x(t) = \Phi(t, t_0) \delta x(t_0) \tag{9}$$

where the differential equation for the state-transition matrix is

$$\dot{\Phi}(t, t_0) = F \Phi(t, t_0), \quad \Phi(t_0, t_0) = I \tag{10}$$

If δV is a correction to a nominal maneuver at time $t^*_{\delta V}$, or if δV is a trajectory correction maneuver (TCM) at time $t^*_{\delta V}$ where the nominal maneuver is zero, the state dispersion at a future time $t > t^*_{\delta V}$ is to first-order given by

$$\delta x(t) = \Phi(t, t^*_{\delta V}) \left[\Phi(t^*_{\delta V}, t_0)\delta x(t_0) + B\delta V\right] \tag{11}$$

$$B = \begin{bmatrix} 0 \\ I \end{bmatrix}$$

In the subsections that follow, the equations of motion above are utilized to derive three impulsive burn targeting algorithms each more general than the previous. Section 4.1 will solve the problem of one impulsive burn and one set of constraints at a single time, Section 4.2 will the solve the problem of one impulsive burn with multiple sets of constraints at multiple times, and Section 4.3 will solve the problem of multiple impulsive burns with multiple sets of constraints at multiple times.

4.1 Single Impulsive Burn with an Arbitrary Number of Constraints at a Single Variable Final Time

This sub-section will outline details for solving the targeting problem for a single impulsive burn with an arbitrary number and type of constraints at a single variable final time. The derivation below is representative for the developments for this section and the subsequent sections. For example, the targeting parameters for this first algorithm are $\delta u = [\delta V, \delta t_f]$ where δV is the deviation of the nominal impulsive burn Δv, and δt_f is deviation of the nominal final constraint time.

Let a single set of targeting constraints at time t_f,$\Psi\left[x(t_f)\right] = 0$, represent m nonlinear constraints that must be satisfied by the final inertial position and velocity state vector $x(t_f)$ at a time $t_f = t^*_f + \delta t_f$, where δt_f can be selected to improve performance. The reference final state vector $x^*(t^*_f)$ at the nominal final time t^*_f, must also satisfy the constraints, $\Psi\left[x^*(t^*_f)\right] = 0$. To first-order, the final state $x(t_f)$ is given by $x(t_f) = x^*(t^*_f) + \delta x(t^*_f) + \dot{x}^*(t^*_f)\delta t_f$, and the m nonlinear constraints can be linearized about the reference position and velocity state vector $x^*(t^*_f)$

$$\Psi\left[x^*(t^*_f)\right] + \left.\frac{\partial \Psi}{\partial x}\right|_{x^*(t^*_f)} \left[\delta x(t^*_f) + \dot{x}^*(t^*_f)\delta t_f\right] \tag{12}$$

or

$$\Psi_{x,f}\left[\delta x(t^*_f) + \dot{x}^*(t^*_f)\delta t_f\right] = 0 \tag{13}$$

where

$$\Psi_{x,f} = \left.\frac{\partial \Psi}{\partial x}\right|_{x^*(t^*_f)}$$

$$\dot{x}^*(t^*_f) = \left.\begin{bmatrix} v^* \\ g(r^*) \end{bmatrix}\right|_{t^*_f}$$

Substituting $\delta t_f = \mathsf{P}^{t_f}_p \delta u$ into Eq. 13 produces

$$\boxed{0 = \Psi_{x,f}\left[\delta x(t^*_f) + \dot{x}^*(t^*_f)\mathsf{P}^{\delta t_f}_{\delta u}\delta u\right]} \tag{14}$$

where $\mathsf{P}^{\delta t_f}_{\delta u}$ represents the partial derivative of δt_f with respect to the targeting parameter vector δu.

The state dispersion $\delta x(t^*_f)$ at time t^*_f is a function of the initial state dispersion, $\delta x(t^*_0)$, and the maneuver impulse, δV, at the fixed maneuver time $t^*_{\delta V}$, and can be found using Eq. 11

$$\delta x(t^*_f) = \Phi(t^*_f, t^*_0)\delta x(t^*_0) + \Phi(t^*_f, t^*_{\delta V})B\delta V$$

or

$$\delta x(t^*_f) = \Phi(t^*_f, t^*_0)\delta x(t^*_0) + \Phi(t^*_f, t^*_{\delta V})B\mathsf{P}^{\delta V}_{\delta u}\delta u \tag{15}$$

where $\mathsf{P}_{\delta u}^{\delta V}$ is the partial derivative of δV with respect to δu.

Eq. 15 can be written in the generic linear form

$$\boxed{\delta x(t_f^*) = M_{x_f x_0}\delta x(t_0^*) + M_{x_f u}\delta u} \tag{16}$$

where

$$M_{x_f x_0} = \Phi(t_f^*, t_0^*)$$

$$M_{x_f u} = \Phi(t_f^*, t_{\delta V}^*)B\mathsf{P}_{\delta u}^{\delta V}$$

Substituting Eq. 16 into the linearized constraints in Eq. 13 produces

$$\boxed{\Psi_{x,f}\left[M_{x_f x_0}\delta x(t_0^*) + \left\{M_{x_f u} + \dot{x}^*(t_f^*)\mathsf{P}_{\delta u}^{\delta t_f}\right\}\delta u\right] = 0}$$

This equation represents m constraint equations in $n = 4$ unknown targeting parameters, δV and δt_f, and can be written in the standard form

$$\boxed{\mathcal{M}\delta u = \mathcal{N}\delta x(t_0^*)} \tag{17}$$

where

$$\mathcal{M} = \ \Psi_{x,f}\left\{M_{x_f u} + \dot{x}^*(t_f^*)\mathsf{P}_{\delta u}^{\delta t_f}\right\} \tag{18}$$

$$\mathcal{N} = - \ \Psi_{x,f}M_{x_f x_0} \tag{19}$$

For fixed final-time problems, the fourth column of $\mathcal{M}$ is removed.

4.2 Single Impulsive Burn with Arbitrary Number of Constraints at Multiple Variable Final Times

In the previous section, the targeting parameters consisted of a single impulsive correction and a single constraint time. The targeting parameters in this section consist of a single corrective impulsive maneuver δV and r variable constraint times $\delta t_{c_i}, i = 1, 2, \cdots, r$, i.e., $\delta u = [\delta V, \Delta T]$ where $\Delta T = [\delta t_{c_1}, \delta t_{c_2}, \ldots, \delta t_{c_r}]$. Let $\Psi_i[x(t_{c_i})] = 0$ represent p_i nonlinear constraints at constraint times $t_{c_i} = t_{c_i}^* + \delta t_{c_i}$, for $i = 1, 2, \ldots, r$, where δt_{c_i} represent r targeting parameters to be determined. The reference state vectors $x^*(t_{c_i}^*)$ at the nominal times $t_{c_i}^*$, must also satisfy the constraints $\Psi_i[x^*(t_{c_i}^*)] = 0$. The total number of constraints is $m = \sum_{i=1}^{r} p_i$.

If the state $x(t_{c_i})$ is expanded to first-order using $x(t_{c_i}) = x^*(t_{c_i}^*) + \delta x(t_{c_i}^*) + \dot{x}^*(t_{c_i}^*)\delta t_{c_i}$, the p_i nonlinear constraints can be linearized about the reference position and velocity state vector $x^*(t_{c_i}^*)$

$$\Psi_i\left[x^*(t_{c_i}^*)\right] + \left.\frac{\partial \Psi_i}{\partial x}\right|_{x^*(t_{c_i}^*)}\left[\delta x(t_{c_i}^*) + \dot{x}^*(t_{c_i}^*)\delta t_{c_i}\right] \tag{20}$$

or

$$0 = \Psi_{x,i}\left[\delta x(t_{c_i}^*) + \dot{x}^*(t_{c_i}^*)\delta t_{c_i}\right], \quad i = 1, 2, \cdots, r \tag{21}$$

where

$$\Psi_{x,i} = \left.\frac{\partial \Psi}{\partial x}\right|_{x^*(t_{c_i}^*)}$$

$$\dot{x}^*(t_{c_i}^*) = \left.\left[\begin{array}{c} v^* \\ g(r^*) \end{array}\right]\right|_{t_{c_i}^*}$$

Substituting $\delta t_{c_i} = \mathsf{P}_{\delta u}^{\delta t_{c_i}}\delta u$, where $\mathsf{P}_{\delta u}^{\delta t_{c_i}}$ represents the partial derivative of δt_{c_i} with respect to the targeting parameter vector δu, produces

$$\boxed{0 = \Psi_{x,i}\left[\delta x(t_{c_i}^*) + \dot{x}^*(t_{c_i}^*)\mathsf{P}_{\delta u}^{\delta t_{c_i}}\delta u\right], \quad i = 1, 2, \cdots, r} \tag{22}$$

As a reminder, each set of constraints $\Psi_{x,i}$ consists of p_i scalar constraints for a total of $m = \sum_{i=1}^{r} p_i$ constraints.

The state dispersion $\delta x(t^*_{c_i})$ in Eq. 21 is a function of the initial state dispersion, $\delta x(t^*_0)$ and the maneuver impulse δV at the fixed maneuver time $t^*_{\delta V}$ and be determined from Eq. 11

$$\delta x(t^*_{c_i}) = \Phi(t^*_{c_i}, t^*_0)\delta x(t^*_0) + \Phi(t^*_{c_i}, t^*_{\delta V})B\delta V$$

or

$$\delta x(t^*_{c_i}) = \Phi(t^*_{c_i}, t^*_0)\delta x(t^*_0) + \Phi(t^*_{c_i}, t^*_{\delta V})B\mathsf{P}^{\delta V}_{\delta u}\delta u, \quad i = 1, 2, \cdots, r \tag{23}$$

where $\mathsf{P}^{\delta V}_{\delta u}$ is the partial derivative of δV with respect to δu.

Eq. 23 can be written in the generic linear form

$$\boxed{\delta x(t^*_{c_i}) = M_{x_{c_i}x_0}\delta x(t^*_0) + M_{x_{c_i}u}\delta u} \tag{24}$$

where

$$M_{x_{c_i}x_0} = \Phi(t^*_{c_i}, t^*_0)$$
$$M_{x_{c_i}u} = \Phi(t^*_{c_i}, t^*_{\delta V})B\mathsf{P}^{\delta V}_{\delta u}$$

Substituting Eq. 24 into the linearized constraints in Eq. 22 produces

$$\boxed{\Psi_{x,i}\left[M_{x_{c_i}x_0}\delta x(t^*_0) + \left\{M_{x_{c_i}u} + \dot{x}^*(t^*_{c_i})\mathsf{P}^{\delta t_{c_i}}_{\delta u}\right\}\delta u\right] = 0} \tag{25}$$

Eq. 25 represents m constraint equations in $n = r + 3$ targeting parameters and can be written in the standard form

$$\boxed{\mathcal{M}\delta u = \mathcal{N}\delta x(t^*_0)} \tag{26}$$

where

$$\mathcal{M} = \begin{bmatrix} \Psi_{x,1}\left\{M_{x_{c_1}u} + \dot{x}^*(t^*_{c_1})\mathsf{P}^{\delta t_{c_1}}_{\delta u}\right\} \\ \Psi_{x,2}\left\{M_{x_{c_2}u} + \dot{x}^*(t^*_{c_2})\mathsf{P}^{\delta t_{c_2}}_{\delta u}\right\} \\ \vdots \\ \Psi_{x,r}\left\{M_{x_{c_r}u} + \dot{x}^*(t^*_{c_r})\mathsf{P}^{\delta t_{c_r}}_{\delta u}\right\} \end{bmatrix} \tag{27}$$

$$\mathcal{N} = -\begin{bmatrix} \Psi_{x,1}M_{x_{c_1}x_0} \\ \Psi_{x,2}M_{x_{c_2}x_0} \\ \vdots \\ \Psi_{x,r}M_{x_{c_r}x_0} \end{bmatrix} \tag{28}$$

These equations represent $m \geq r$ constraints (at least one scalar constraint at each of the r variable constraint times t_{c_i}) and $r + 3$ unknowns (one δV vector and the r time variations, δt_{c_i}). Constraints can be added or removed by adding or deleted the associated rows from $\mathcal{M}$ and $\mathcal{N}$. Fixed constraint time problems can be handled by removing $\dot{x}^*(t^*_{c_i})$ from $\mathcal{M}$ and the associated column from $M_{x_{c_i}u}$.

4.3 Multiple Burns with Arbitrary Number of Constraints at Multiple Fixed or Variable Final Times

The previous section introduced an arbitrary number of sets of constraints at multiple constraint times $t^*_{c_i}$. The same constraints will be applied here, but q multiple impulsive maneuvers δV_j will now be allowed at fixed maneuver times, $t^*_{\delta v_j}, j = 1, 2, \cdots q$. The targeting parameters for this targeting algorithm are $\delta u = [\Delta V, \Delta T]$ and consists of q impulsive maneuvers $\Delta V = [\delta V_1, \delta V_{2,} \ldots, \delta V_q]$, and r constraint times $\Delta T = [\delta t_{c_1}, \delta t_{c_2}, \ldots, \delta t_{c_r}]$.

The linearized constraints in Eq. 22 are repeated here for convenience.

$$\boxed{0 = \Psi_{x,i}\left[\delta x(t^*_{c_i}) + \dot{x}^*(t^*_{c_i})\mathsf{P}^{\delta t_{c_i}}_{\delta u}\,\delta u\right], \quad i = 1, 2, \cdots, r} \tag{29}$$

where$\mathsf{P}^{\delta t_{c_i}}_{\delta u}$ represents the partial derivative of δt_{c_i} with respect to the targeting parameter vector δu. As a reminder, each set of constraints Ψ_i consists of p_i scalar constraints for a total of $m = \sum_{i=1}^{r} p_i$ constraints.

The state dispersion at each of the constraint times $\delta x(t^*_{c_i})$ in Eq. 29 can be determined by repeated applications of Eq. 11 and is a function of the initial state dispersion, $\delta x(t^*_0)$, and the maneuver impulses δV_j at the fixed maneuver times, $t_{\Delta v_j} < t^*_{c_i}, j = 0, 1, \cdots q_i$. It is assumed there are q_1 maneuver impulses from t_0 to t_{c_1}, q_2 maneuver impulses from t_0 to t_{c_2}, etc., such that a total of $q = q_r$ maneuver impulses are allowed from t_0 to t_{c_r}. Using this maneuver numbering scheme, the state dispersion $\delta x(t^*_{c_i})$, at times $t^*_{c_i}$, $i = 1, 2, \cdots r$, are given by

$$\delta x(t^*_{c_2}) = \Phi(t^*_{c_1}, t^*_0)\delta x(t^*_0) + \sum_{j=0}^{q_1} \Phi(t^*_{c_1}, t^*_{\delta V_j})B\delta V_j$$

$$\delta x(t^*_{c_2}) = \Phi(t^*_{c_2}, t^*_0)\delta x(t^*_0) + \sum_{j=0}^{q_2} \Phi(t^*_{c_2}, t^*_{\delta V_j})B\delta V_j,$$

$$\vdots$$

$$\delta x(t^*_{c_r}) = \Phi(t^*_{c_r}, t^*_0)\delta x(t^*_0) + \sum_{j=0}^{q=q_r} \Phi(t^*_{c_r}, t^*_{\delta V_j})B\delta V_j,$$

or in a more compact form

$$\delta x(t^*_{c_i}) = \Phi(t^*_{c_i}, t^*_0)\delta x(t^*_0) + \left[\sum_{j=0}^{q=q_i} \Phi(t^*_{c_i}, t^*_{\delta V_j})B\mathsf{P}^{\delta V_j}_{\delta u}\right]\delta u, \quad i = 1, 2, \cdots, r \tag{30}$$

where $\mathsf{P}^{\delta V_j}_{\delta u}$ is the partial derivative of δV_j with respect to δu.

Eq. 30 can be written in the generic linear form

$$\boxed{\delta x(t^*_{c_i}) = M_{x_{c_i}x_0}\delta x(t^*_0) + M_{x_{c_i}u}\delta u} \tag{31}$$

where

$$M_{x_{c_i}x_0} = \Phi(t^*_{c_i}, t^*_0)$$

$$M_{x_{c_i}u} = \left[\sum_{j=0}^{q=q_i} \Phi(t^*_{c_i}, t^*_{\delta V_j})B\mathsf{P}^{\delta V_j}_{\delta u}\right]$$

Substituting Eq. 31 into the linearized constraints in Eq. 29 produces

$$\boxed{\Psi_{x,i}\left[M_{x_{c_i}x_0}\delta x(t^*_0) + \left\{M_{x_{c_i}u} + \dot{x}^*(t^*_{c_i})\mathsf{P}^{\delta t_{c_i}}_{\delta u}\right\}\delta u\right] = 0}$$

The equation above represents m constraint equations in n targeting parameters and can be written in the standard form

$$\boxed{\mathcal{M}\delta u = \mathcal{N}\delta x(t^*_0)} \tag{32}$$

where

$$\mathcal{M} = \begin{bmatrix} \Psi_{x,1}\left\{M_{x_{c_1}u} + \dot{x}^*(t^*_{c_1})\mathsf{P}^{\delta t_{c_1}}_{\delta u}\right\} \\ \Psi_{x,2}\left\{M_{x_{c_2}u} + \dot{x}^*(t^*_{c_2})\mathsf{P}^{\delta t_{c_2}}_{\delta u}\right\} \\ \vdots \\ \Psi_{x,r}\left\{M_{x_{c_r}u} + \dot{x}^*(t^*_{c_r})\mathsf{P}^{\delta t_{c_r}}_{\delta u}\right\} \end{bmatrix} \tag{33}$$

$$\mathcal{N} = -\begin{bmatrix} \Psi_{x,1}M_{x_{c_1}x_0} \\ \Psi_{x,2}M_{x_{c_2}x_0} \\ \vdots \\ \Psi_{x,r}M_{x_{c_r}x_0} \end{bmatrix} \tag{34}$$

These equations represent $m \geq r$ constraints (at least one scalar constraint at each of the r variable constraint times t_{c_i}) and $3q + r$ unknowns (q Δv vectors and the r time variations, δt_{c_i}). Constraints can be added or removed by adding or deleted the associated rows from $\mathcal{M}$ and $\mathcal{N}$. Fixed constraint time problems can be handled by removing $\dot{x}^*(t^*_{c_i})$ from $\mathcal{M}$ and the associated column from $M_{x_{c_i}u}$.

5 GRT USING FINITE BURNS WITH VARYING THRUST VECTOR

The objective of this section is to derive an implementation of GRT using finite burns with a varying thrust vector that determines the values of up to $n = 6$ targeting parameters to achieve a set of m constraints at a variable final time. Underlying the derivation is the assumption that a reference trajectory that satisfies the final constraints exists. The reference trajectory consists of a coasting-flight, powered-flight, and final coasting-flight segments as notionally shown in Figure 2. This finite burn implementation of GRT uses a constant perturbation to the nominal thrust vector as a targeting parameter such that the total $n = 6$ number of target parameters are $\delta u = [\delta T, \delta t_{tig}, \delta t_{co}, \delta t_f]$, to achieve a set of m constraints at a variable final time.

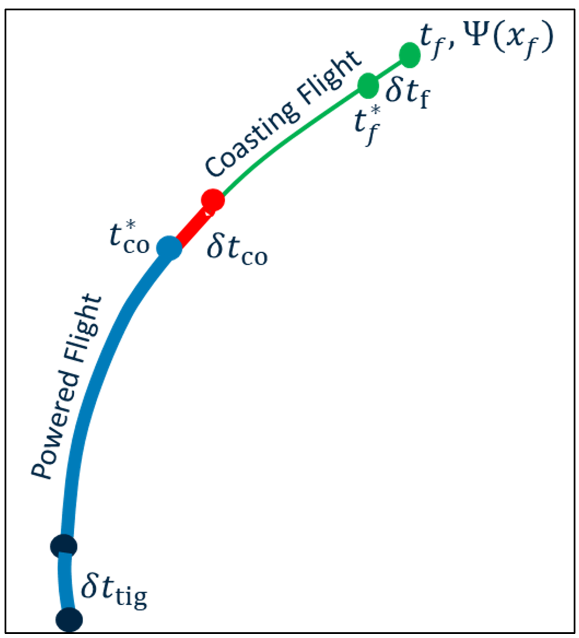

Figure 2. Notional Finite Burn Reference Trajectory.

In Section 5.1 the nonlinear powered-flight equations of motion are presented and linearized about a reference trajectory. In Section 5.2 a state-space targeting model is introduced that includes both the targeting algorithm parameters and the linearized powered-flight equations of motion. This model is presented in terms of matrix block partitions explicitly showing the dependency of the powered-flight equations on the targeting parameters. In Section 5.3 the targeting model state-transition matrix is used to relate initial trajectory dispersion and targeting parameters to the final state dispersion, and lastly, in Section 5.4 the nonlinear constraints on the final state dispersion are introduced and linearized about the reference trajectory. The targeting model STM and the linearized targeting constraint equations are then used to solve for the values of the targeting parameters required to achieve the targeting constraints.

5.1 Powered-Flight Dynamics

The nonlinear powered-flight dynamics are written in terms of the inertial position $r(t)$ and velocity $v(t)$, the mass of the vehicle $m(t)$, the thrust vector $T(t)$, and the thrust efficiency α=constant (defined as one divided by the engine exhaust velocity). The relevant nonlinear differential equations are

$$\dot{r} = v \tag{35}$$

$$\dot{v} = g(r) + \frac{T}{m} \tag{36}$$

$$\dot{m} = -\|T\|\,\alpha \tag{37}$$

$$\dot{\alpha} = 0 \tag{38}$$

If the reference trajectory is defined by $r^*(t)$, $v^*(t)$, $m^*(t)$, α^*, and the nominal thrust vector is defined by T^*, the above equations can be linearized about the reference values and written in terms of the trajectory dispersion $\delta x = [\delta r, \delta v, \delta m, \delta\alpha]^T$, and a thrust vector perturbation δT. The associated linearized differential equations are then given by

$$\dot{\delta r} = \delta v \tag{39}$$

$$\dot{\delta v} = G\delta r + M\delta m + \Lambda\delta T \tag{40}$$

$$\dot{\delta m} = -\|T^*\|\,\delta\alpha + \Gamma\delta T \tag{41}$$

$$\dot{\delta \alpha} = 0 \tag{42}$$

where

$$G = \left.\frac{\partial g(r)}{\partial r}\right|_* \tag{43}$$

$$M = -\frac{T^*}{(m^*)^2} \tag{44}$$

$$\Lambda = \frac{1}{m^*} \tag{45}$$

$$\Gamma = -\alpha^* i_{T^*}^T \tag{46}$$

where $i_{T^*} = T^*/\,\|T^*\|$.

In the models developed below the time-derivative of the reference state vector during powered-flight (indicated by a subscript T) is given by

$$\dot{x}_T^* = \begin{bmatrix} v^* \\ g(r^*) + \frac{T^*}{m^*} \\ -\|T^*\|\,\alpha^* \\ 0 \end{bmatrix} \tag{47}$$

and the time-derivative of the reference state vector is during coasting-flight (indicated by a subscript C) is given by

$$\dot{x}_C^* = \begin{bmatrix} v^* \\ g(r^*) \\ 0 \\ 0 \end{bmatrix} \tag{48}$$

5.2 Targeting Model Dynamics

The state vector for the targeting model dynamics is obtained by appending the targeting six parameters $\delta u = [\delta T, \delta t_f, \delta t_{tig}, \delta t_{co}]$ to powered-flight state vector $\delta x = [\delta r, \delta v, \delta m, \delta\alpha]^T$, such that

$$\delta x_{tgt} = \begin{bmatrix} \delta x \\ \delta u \end{bmatrix}$$

where the targeting model dynamics are given by

$$\begin{aligned} \dot{\delta r} &= \delta v && (49) \\ \dot{\delta v} &= G\delta r + M\delta m + \Lambda\delta T && (50) \\ \dot{\delta m} &= -\|T^*\|\,\delta\alpha - \Gamma\delta T && (51) \\ \dot{\delta\alpha} &= 0 && (52) \\ \dot{\delta T} &= 0 && (53) \\ \dot{\delta t_f} &= 0 && (54) \\ \dot{\delta t_{tig}} &= 0 && (55) \\ \dot{\delta t_{co}} &= 0 && (56) \end{aligned}$$

or

$$\delta\dot{x}_{tgt} = F_{tgt}(t)\delta x_{tgt}$$

where the Jacobian $F_{tgt}(t)$ can be written in terms of matrix block partitions

$$F_{tgt}(t) = \begin{bmatrix} F_{xx} & F_{xu} \\ 0_{6\times 8} & 0_{6\times 6} \end{bmatrix}\Bigg|_* \tag{57}$$

$$F_{xx}(t) = \begin{bmatrix} 0_{3\times 3} & I_{3\times 3} & 0_{3\times 1} & 0_{3\times 1} \\ G & 0_{3\times 3} & M & 0_{3\times 1} \\ 0_{1\times 3} & 0_{1\times 3} & 0 & -\|T^*\| \\ 0_{1\times 3} & 0_{1\times 3} & 0_{1\times 1} & 0_{1\times 1} \end{bmatrix} \tag{58}$$

$$F_{xu}(t) = \begin{bmatrix} 0_{3\times 3} & 0_{3\times 3} \\ \Lambda & 0_{3\times 3} \\ \Gamma & 0_{1\times 3} \\ 0_{1\times 3} & 0_{1\times 3} \end{bmatrix} \tag{59}$$

and where $T^* = M = \Lambda = \Gamma = 0$ during coasting-flight.

Similarly, in discrete-time the STM can be written in terms of matrix block partitions,

$$\Phi_{tgt}(t, t_0) = \begin{bmatrix} \Phi_{xx} & \Phi_{xu} \\ 0 & I \end{bmatrix}\Bigg|_* \tag{60}$$

where the STM is determined by numerically integrating

$$\dot{\Phi}_{tgt}(t, t_0) = F_{tgt}(t)\Phi_{tgt}(t, t_0), \quad \Phi_{tgt}(t_0, t_0) = I$$

5.3 Relating Targeting Parameters to Final Trajectory Dispersion

To first order, the targeting state dispersion at the end of the first coasting-flight segment and at the nominal time of engine ignition t^*_{tig} is a function of the initial targeting state dispersion, $\delta x_{tgt}(t^*_0)$, and the time-of-ignition dispersion, δt_{tig},

$$\delta x_{tgt}(t^*_{tig}) = \Phi_{tgt}(t^*_{tig}, t^*_0)\delta x_{tgt}(t^*_0) + \left[\dot{x}^*_{tgt,C}(t^*_{tig}) - \dot{x}^*_{tgt,T}(t^*_{tig})\right]\delta t_{tig} \tag{61}$$

where $\dot{x}^*_{tgt,C}(t^*_{tig})$ is the reference state time-derivative at the end of the coasting-flight (C) segment given in Eq. 48 appended with zeros to accommodate constant targeting parameters states, and $\dot{x}^*_{tgt,T}(t^*_{tig})$ is the reference state time-derivative at the beginning of the powered-flight (T) segment given in Eq. 47, again appended with zeros to accommodate the constant targeting parameters states. Eq. 61 can be written as

$$\delta x_{tgt}(t^*_{tig}) \quad = \quad \left[\Phi_{tgt}(t^*_{tig}, t^*_0) + \Delta\dot{x}^*_{tgt}(t^*_{tig})\mathsf{P}^{\delta t_{tig}}_{\delta x_{tgt}}\right] \delta x_{tgt}(t^*_0) \tag{62}$$

where $\mathsf{P}^{\delta t_{tig}}_{\delta x_{tgt}}$ is the partial derivative of δt_{tig} with respect to the targeting model state vector vector δx_{tgt}, and $\Delta\dot{x}^*_{tgt}(t^*_{tig}) = \dot{x}^*_{tgt,C}(t^*_{tig}) - \dot{x}^*_{tgt,T}(t^*_{tig})$.

Next, the targeting model state dispersion at the nominal engine cutoff time t^*_{co} is, to first-order, a function of the targeting state dispersion at the nominal time-of-ignition, $\delta x_{tgt}(t^*_{tig})$, and the engine cutoff time dispersion, δt_{co},

$$\delta x_{tgt}(t^*_{co}) \quad = \quad \Phi_{tgt}(t^*_{co}, t^*_{tig})\delta x_{tgt}(t^*_{tig}) + \left[\dot{x}^*_{tgt,T}(t^*_{co}) - \dot{x}^*_{tgt,C}(t^*_{co})\right] \delta t_{co} \tag{63}$$

where$\dot{x}^*_{tgt,T}(t^*_{co})$ and $\dot{x}^*_{tgt,C}(t^*_{co})$ are the state time-derivatives at the nominal time of engine cut-off. Eq. 63 can be written as

$$\delta x_{tgt}(t^*_{co}) \quad = \quad \Phi_{tgt}(t^*_{co}, t^*_{tig})\delta x_{tgt}(t^*_{tig}) - \Delta\dot{x}^*_{tgt}(t^*_{co})\mathsf{P}^{\delta t_{co}}_{\delta x_{tgt}}\delta x_{tgt}(t^*_0) \tag{64}$$

where $\mathsf{P}^{\delta t_{co}}_{\delta x_{tgt}}$ is the partial derivative of δt_{co} with respect to the targeting model state vector δx_{tgt} .

Lastly, the targeting model state dispersion at the nominal final time and end of the final coast segment, $\delta x(t^*_f)$ is given by

$$\delta x_{tgt}(t^*_f) \quad = \quad \Phi_{tgt}(t^*_f, t^*_{co})\delta x_{tgt}(t^*_{co}) \tag{65}$$

Substituting 62 into 64, and 64 into 65, produces

$$\delta x_{tgt}(t^*_f) \quad = \quad \Phi_{tgt}(t^*_f, t^*_{co}) \left\{\Phi_{tgt}(t^*_{co}, t^*_{tig}) \left[\Phi_{tgt}(t^*_{tig}, t^*_0) + \Delta\dot{x}^*_{tgt}(t^*_{tig})\mathsf{P}^{\delta t_{tig}}_{\delta x_{tgt}}\right] - \Delta\dot{x}^*_{tgt}(t^*_{co})\mathsf{P}^{\delta t_{co}}_{\delta x_{tgt}}\right\} \delta x_{tgt}(t^*_0)$$

Since Φ_{tgt} has the matrix block partition form shown in Eq. 60, and since the time-derivative of the reference targeting state vector has the form,

$$\delta\dot{x}^*_{tgt} = \begin{bmatrix} \delta\dot{x}^* \\ \delta\dot{u}^* \end{bmatrix} = \begin{bmatrix} \delta\dot{x}^* \\ 0_{7\times1} \end{bmatrix}$$

Eq. 66 can be written in terms of matrix block partitions

$$\delta x_{tgt}(t^*_f) \quad = \quad \begin{bmatrix} M_{xx} & M_{xu} \\ 0 & I \end{bmatrix} \delta x_{tgt}(t^*_0) \tag{66}$$

$$\boxed{\delta x(t^*_f) = M_{xx}\delta x(t^*_0) + M_{xu}\delta u} \tag{67}$$

$$\delta u(t^*_f) = \delta u \tag{68}$$

where

$$M_{xx} = \Phi_{xx}(t^*_f, t^*_0) \tag{69}$$

$$M_{xu} = \Phi_{xx}(t^*_f, t^*_{co}) \left[\Phi_{xx}(t^*_{co}, t^*_{tig})\Delta\dot{x}^*_{tgt}(t^*_{tig})\mathsf{P}^{\delta t_{tig}}_{\delta u} - \Delta\dot{x}^*_{tgt}(t^*_{co})\mathsf{P}^{\delta t_{co}}_{\delta u}\right] + \Phi_{xu}(t^*_f, t^*_0) \tag{70}$$

where the Jacobian and state-transition matrix are now defined by Eqs. 57-60.

As expected, Eq. 68 shows that the targeting parameters δu are constant, and Eq. 67 shows how the initial state dispersion $\delta x(t^*_0)$ and the targeting parameters δu contribute to the final dispersion $\delta x(t^*_f)$, or, in other words, given an initial state dispersion, $\delta x(t^*_0)$, Eq. 67 provides the information needed to compute the values of the targeting parameters δu required to achieve the desired final dispersion constraints. This last step will be presented in the next section.

5.4 Trajectory Constraints and Targeting Solution

Let $\Psi\left[x(t_f)\right] = 0$ represent m nonlinear constraints that must be satisfied by the final state vector $x(t_f)$ at a time $t_f = t_f^* + \delta t_f$, where δt_f is a variable final constraint time determined by the targeting algorithm. The reference final state vector $x^*(t_f^*)$ at the nominal final time t_f^*, must also satisfy the constraints, i.e., $\Psi\left[x^*(t_f^*)\right] = 0$. If the final state $x(t_f)$ is to first-order given by $x(t_f) = x^*(t_f^*) + \delta x(t_f^*) + \dot{x}_C^*(t_f^*)\delta t_f$, the m nonlinear constraints can be linearized about the reference state vector $x^*(t_f^*)$

$$\Psi\left[x^*(t_f^*)\right] + \left.\frac{\partial \Psi}{\partial x}\right|_{x^*(t_f^*)} \left[\delta x(t_f^*) + \dot{x}_C^*(t_f^*)\delta t_f\right] \tag{71}$$

or

$$0 = \Psi_{x,f}\left[\delta x(t_f^*) + \dot{x}_C^*(t_f^*)\delta t_f\right] \tag{72}$$

where

$$\Psi_{x,f} = \left.\frac{\partial \Psi}{\partial x}\right|_{x^*(t_f^*)}$$

Substituting $\delta t_f = \mathsf{P}_{\delta u}^{\delta t_f}\delta u$ in Eq. 72 produces

$$\boxed{0 = \Psi_{x,f}\left[\delta x(t_f^*) + \dot{x}^*(t_f^*)\mathsf{P}_{\delta t_f,\delta u}\delta u\right]} \tag{73}$$

where $\mathsf{P}_{\delta u}^{\delta t_f}$ represents the partial derivative of δt_f with respect to the targeting parameter vector δu.

Substituting Eq. 67 into Eq. 73 produces

$$\boxed{0 = \Psi_{x,f}\left[M_{xx}\delta x(t_0^*) + \left\{M_{xu} + \dot{x}_C^*(t_f^*)\mathsf{P}_{\delta u}^{\delta t_f}\right\}\delta u\right]}$$

which results in m algebraic equations in $n = 6$ unknowns

$$\boxed{\mathcal{M}\delta u = \mathcal{N}\delta x(t_0^*)} \tag{74}$$

$$\mathcal{M} = \Psi_{x,f}\left\{M_{xu} + \dot{x}_C^*(t_f^*)\mathsf{P}_{\delta u}^{\delta t_f}\right\}$$
$$\mathcal{N} = -\Psi_{x,f}M_{xx}$$

where M_{xx} and M_{xu} are given in Eqs. 69 and 69 and defined by the new Jacobian and state-transition matrix.

Eq. 74 represents the solution to this finite-burn targeting problem. There are m constraint equations in 6 unknown targeting parameters, δT, δt_{tig}, δt_{co} and δt_f. When constraints are added or removed from the targeting problem, the corresponding rows of $\mathcal{M}$ and $\mathcal{N}$ are added or removed. If fewer parameters are required, the corresponding columns of $\mathcal{M}$ are removed.

Further, when the only targeting parameter is the perturbation to the thrust vector δT, the above matrices reduce to

$$\mathcal{M} = \Psi_{x_f}\Phi_{xu}(t_f^*, t_0^*)$$
$$\mathcal{N} = -\Psi_{x_f}\Phi_{xx}(t_f^*, t_0^*)$$

6 GRT USING FINITE BURNS WITH FIXED THRUST MAGNITUDE

In this section an alternative to the finite burn GRT implementation in Section 5 is presented. The powered-flight dynamics are the same as in the previous section, however a different set of targeting parameters is utilized. Instead of using a constant perturbation to the nominal thrust vector, this modified finite burn implementation of GRT uses a constant perturbation to the initial thrust direction and turning rate assuming a fixed thrust magnitude. Consequently, instead of 6 targeting parameters, this formulation has $n = 7$ targeting parameters, $\delta u = [\delta b, \delta g, \delta t_{tig}, \delta t_{co}, \delta t_f]$ where δb is a perturbation to the initial thrust direction , δg is a constant perturbation to the thrust turning rate, and δt_{tig}, δt_{co} and δt_f are perturbations to the engine ignition time, engine cutoff time, and the final constraint time, respectively. The perturbations to the initial thrust direction and turning rate are 2-dimensional and are constrained to be perpendicular to the initial nominal thrust direction. The objective of this section is to derive an algorithm that can determine the values of the targeting parameters needed to achieve a set of m constraints. The remainder of this section follows the same approach as in Section 5.

In Section 5.1 the nonlinear powered-flight equations of motion are presented and linearized about a reference trajectory. In Section 5.2 a state-space targeting model is introduced that includes both the targeting algorithm parameters and the linearized powered-flight equations of motion. This model is presented in terms of matrix block partitions explicitly showing the dependency of the powered-flight equations on the targeting parameters. In Section 5.3 the targeting model state-transition matrix is used to relate initial trajectory dispersion and targeting parameters to the final state dispersion, and lastly, in Section 5.4 the nonlinear constraints on the final state dispersion are introduced and linearized about the reference trajectory. The targeting model STM and the linearized targeting constraint equations are then used to solve for the values of the targeting parameters required to achieve the targeting constraints.

6.1 Powered-Flight Dynamics

The nonlinear powered-flight dynamics are written in terms of the inertial position $r(t)$ and velocity $v(t)$, the mass of the vehicle $m(t)$, the thrust magnitude $T(t)$, the thrust efficiency α=constant (defined as one divided by the engine exhaust velocity), and the thrust direction $\lambda(t)$. The relevant nonlinear differential equations are

$$\dot{r} = v \tag{75}$$

$$\dot{v} = g(r) + \frac{T}{m}\frac{\lambda}{||\lambda||} \tag{76}$$

$$\dot{m} = -T\alpha \tag{77}$$

$$\dot{\alpha} = 0 \tag{78}$$

If the reference trajectory is defined by $r^*(t)$, $v^*(t)$, $m^*(t)$, α^*, and the nominal thrust vector is defined by $T^*\hat{\lambda}^*(t)$, the above equations can be linearized about the reference values and written in terms of the trajectory dispersions $\delta r(t)$, $\delta v(t)$, $\delta m(t)$, $\delta\alpha(t)$, and a thrust vector perturbation $\delta\lambda(t) = \delta\beta + \delta\gamma(t - t^*_{tig})$, where $\delta\beta$, and $\delta\gamma$ are constants. The associated linearized differential equations are then given by

$$\dot{\delta r} = \delta v \tag{79}$$

$$\dot{\delta v} = G\delta r + M\delta m + \Lambda\delta\beta + \Gamma\delta\gamma \tag{80}$$

$$\dot{\delta m} = -T^*\delta\alpha \tag{81}$$

$$\dot{\delta\alpha} = 0 \tag{82}$$

$$\dot{\delta\beta} = 0 \tag{83}$$

$$\dot{\delta\gamma} = 0 \tag{84}$$

where

$$G = \left.\frac{\partial g(r)}{\partial r}\right|_* \tag{85}$$

$$M = -\frac{T^*}{m^2}\frac{\lambda^*}{||\lambda^*||} \tag{86}$$

$$\Lambda = \frac{T^*}{m}\frac{1}{||\lambda^*||}\left[I - \frac{\lambda^*}{||\lambda^*||}\frac{\lambda^{*T}}{||\lambda^*||}\right] \tag{87}$$

$$\Gamma = \Lambda(t - t^*_{tig}) \tag{88}$$

Although the trajectory dispersions are assumed to be small, they are generally unconstrained. However, the initial thrust direction perturbation $\delta\beta$ and turning rate $\delta\gamma$ are required to be perpendicular to the nominal initial thrust $\lambda^*_{tig} = \lambda^*(t^*_{tig})$. To enforce this constraint, the perturbation $\delta\beta$ is written as

$$\delta\beta = \delta b_1 \hat{\lambda}^*_{\perp_1} + \delta b_2 \hat{\lambda}^*_{\perp_2} \tag{89}$$

$$\delta\beta = \begin{bmatrix} \hat{\lambda}^*_{\perp_1} & \hat{\lambda}^*_{\perp_2} \end{bmatrix} \begin{bmatrix} \delta b_1 \\ \delta b_2 \end{bmatrix} \tag{90}$$

$$\delta\beta = L\delta b \tag{91}$$

where

$$\hat{\lambda}^*_{\perp_1} = \frac{\hat{\lambda}^*_{tig} \times \hat{i}_z}{||\hat{\lambda}^*_{tig} \times \hat{i}_z||} \tag{92}$$

$$\hat{\lambda}^*_{\perp_2} = \frac{\hat{\lambda}^*_{tig} \times \hat{\lambda}^*_{\perp_1}}{||\hat{\lambda}^*_{tig} \times \hat{\lambda}^*_{\perp_1}||} \tag{93}$$

Similarly, the turning rate perturbation $\delta\gamma$ is written as

$$\delta\gamma = \delta g_1 \hat{\lambda}^*_{\perp_1} + \delta g_2 \hat{\lambda}^*_{\perp_2} \tag{94}$$

$$\delta\gamma = \begin{bmatrix} \hat{\lambda}^*_{\perp_1} & \hat{\lambda}^*_{\perp_2} \end{bmatrix} \begin{bmatrix} \delta g_1 \\ \delta g_2 \end{bmatrix} \tag{95}$$

$$\delta\gamma = L\delta g \tag{96}$$

Using this formulation for the thrust vector perturbation, the linearized equations of motion in terms of the state vector perturbation $\delta x = [\delta r, \delta v, \delta m, \delta\alpha]^T$ are given by

$$\dot{\delta r} = \delta v \tag{97}$$

$$\dot{\delta v} = G\delta r + M\delta m + \Lambda L \delta b + \Gamma L \delta g \tag{98}$$

$$\dot{\delta m} = -T^* \delta\alpha \tag{99}$$

$$\dot{\delta\alpha} = 0 \tag{100}$$

where during powered-flight (T) the time-derivative of the reference state vector is given by

$$\dot{x}^*_T = \begin{bmatrix} v^* \\ g(r^*) + \frac{T^*}{m^*}\frac{\lambda^*}{||\lambda^*||} \\ -T^*\alpha^* \\ 0 \end{bmatrix} \tag{101}$$

and during coasting-flight (C) the time-derivative of the reference state vector dynamics is

$$\dot{x}^*_C = \begin{bmatrix} v^* \\ g(r^*) \\ 0 \\ 0 \end{bmatrix} \tag{102}$$

6.2 Targeting Model Dynamics

The state vector for the targeting model dynamics is obtained by appending the targeting parameters $\delta u = [\delta b, \delta g, \delta t_{tig}, \delta t_{co}, \delta t_f]$ to powered-flight state vector $\delta x = [\delta r, \delta v, \delta m, \delta\alpha]^T$, i.e.

$$\delta x_{tgt} = \begin{bmatrix} \delta x \\ \delta u \end{bmatrix}$$

where the targeting model dynamics are given by

$$\begin{aligned}
\dot{\delta r} &= \delta v && (103)\\
\dot{\delta v} &= G\delta r + M\delta m + \Lambda L\delta b + \Gamma L\delta g && (104)\\
\dot{\delta m} &= -T\delta\alpha && (105)\\
\dot{\delta \alpha} &= 0 && (106)\\
\dot{\delta b} &= 0 && (107)\\
\dot{\delta g} &= 0 && (108)\\
\dot{\delta t_{tig}} &= 0 && (109)\\
\dot{\delta t_{co}} &= 0 && (110)\\
\dot{\delta t_{f}} &= 0 && (111)
\end{aligned}$$

or

$$\delta\dot{x}_{tgt} = F_{tgt}(t)\delta x_{tgt}$$

where the Jacobian $F_{tgt}(t)$ can be written in terms of matrix block partitions

$$F_{tgt}(t) = \left.\begin{bmatrix} F_{xx} & F_{xu} \\ 0_{7\times 8} & 0_{7\times 7} \end{bmatrix}\right|_{*} \tag{112}$$

$$F_{xx}(t) = \left.\begin{bmatrix} 0_{3\times 3} & I_{3\times 3} & 0_{3\times 1} & 0_{3\times 1} \\ G & 0_{3\times 3} & M & 0_{3\times 1} \\ 0_{1\times 3} & 0_{1\times 3} & 0 & -T \\ 0_{1\times 3} & 0_{1\times 3} & 0_{1\times 1} & 0_{1\times 1} \end{bmatrix}\right|_{*} \tag{113}$$

$$F_{xu}(t) = \left.\begin{bmatrix} 0_{3\times 2} & 0_{3\times 2} & 0_{3\times 3} \\ \Lambda L & \Gamma L & 0_{3\times 3} \\ 0_{1\times 2} & 0_{1\times 2} & 0_{1\times 3} \\ 0_{1\times 2} & 0_{1\times 2} & 0_{1\times 3} \end{bmatrix}\right|_{*} \tag{114}$$

and where $T = M = \Lambda = \Gamma = 0$ during coasting-flight.

Similarly, in discrete-time the STM can be written in terms of matrix block partitions,

$$\Phi_{tgt}(t, t_0) = \left.\begin{bmatrix} \Phi_{xx} & \Phi_{xu} \\ 0 & I \end{bmatrix}\right|_{*} \tag{115}$$

where the STM can be determined numerically by integrating

$$\dot{\Phi}_{tgt}(t, t_0) = F_{tgt}(t)\Phi_{tgt}(t, t_0), \quad \Phi_{tgt}(t_0, t_0) = I$$

6.3 Relating Targeting Parameters to Final Trajectory Dispersion

The approach to relating targeting parameters to the final trajectory dispersion is identical to the approach in Section 5.3, and the final result is the same,

$$\boxed{\delta x(t_f^*) = M_{xx}\delta x(t_0^*) + M_{xu}\delta u} \tag{116}$$

$$M_{xx} = \Phi_{xx}(t_f^*, t_0^*)$$

$$M_{xu} = \Phi_{xx}(t_f^*, t_{co}^*)\left[\Phi_{xx}(t_{co}^*, t_{tig}^*)\Delta\dot{x}_{tgt}^*(t_{tig}^*)\mathsf{P}_{\delta u}^{\delta t_{tig}} - \Delta\dot{x}_{tgt}^*(t_{co}^*)\mathsf{P}_{\delta u}^{\delta t_{co}}\right] + \Phi_{xu}(t_f^*, t_0^*)$$

where the Jacobian and state-transition matrix are now defined by Eqs. 112-115.

6.4 Trajectory Constraints and Targeting Solution

Similarly, the approach to deriving the final targeting solution is same as in Section 5.4 , and the final result is identical,

$$\boxed{\mathcal{M}\delta u = \mathcal{N}\delta x(t_0^*)} \tag{117}$$

where

$$\mathcal{M} = \Psi_{x,f}\left\{M_{xu} + \dot{x}_C^*(t_f^*)\mathsf{P}_{\delta u}^{\delta t_f}\right\}$$

$$\mathcal{N} = -\Psi_{x,f}M_{xx}$$

Eq. 117 represents the solution to this finite-burn targeting problem. There are m constraint equations and 7 unknown targeting parameters, $\delta c = [\delta c_1, \delta c_2]^T$, $\delta g = [\delta g_1, \delta g_2]^T$, δt_{tig}, δt_{co}, and δt_f. When constraints are added or removed from the targeting problem, the corresponding rows of $\mathcal{M}$ and $\mathcal{N}$ are added or removed. If fewer parameters are required, the corresponding columns of $\mathcal{M}$ are removed.

Further, when the only targeting parameters are the perturbation to the initial thrust direction and thrust turning rate, the above matrices reduce to

$$\mathcal{M} = \Psi_{x_f}\Phi_{xu}(t_f^*, t_0^*)$$

$$\mathcal{N} = -\Psi_{x_f}\Phi_{xx}(t_f^*, t_0^*)$$

7 GRT FOR DUAL INERTIAL RELATIVE TARGETING

The above targeting formulations were focused on solving problems with constraints on the inertial position and velocity of a single vehicle, such as the absolute trajectory constraints. In this section, the above targeting solutions are reused to solve problems with relative trajectory constraints such as specifying limits on the relative position and velocity of two vehicles.

Let x_1 denote the inertial position r_1 and velocity v_1 of an active Vehicle 1 with impulsive or finite maneuver capability. This is the same inertial position/velocity state used to develop the absolute targeting algorithms above. For finite-burns/powered-flight x_1 also includes mass m_1 and thrust efficiency α_1. Let x_2 denote the inertial position r_2 and velocity v_2 of a passive Vehicle 2. Let $x = [x_1, x_2]$ denote a dual-inertial state vector, and let the relative position and velocity state be denoted by $x_{rel} = [r_1 - r_2, v_1 - v_2] = M_{rel}x$ where M_{rel} maps the absolute positions and velocities of Vehicles 1 and 2 to the relative position and velocity. The reference trajectories for Vehicles 1 and 2 are denoted by x_1^* and x_2^*, and the relative reference trajectory is denoted by x_{rel}^*.

The relative trajectory constraints, $\Psi_i[x_{rel}(t_{c_i})] = 0$, represent p_i nonlinear constraints at times $t_{c_i} = t_{c_i}^* + \delta t_{c_i}$, for $i = 1, 2, \ldots, r$, where the δt_{c_i}represent r targeting parameters, $\delta T = [\delta t_{c_1}, \delta t_{c_2}, \ldots, \delta t_{c_r}]$, to be determined. The reference relative state vectors $x^*(t_{c_i}^*)$ at the nominal times $t_{c_i}^*$, must also satisfy the relative constraints $\Psi_i[x_{rel}^*(t_{c_i}^*)] = 0$. The total number of constraints is $m = \sum_{i=1}^r p_i$.

If the relative state $x_{rel}(t_{c_i})$ is expanded to first-order using $x_{rel}(t_{c_i}) = x_{rel}^*(t_{c_i}^*) + \delta x_{rel}(t_{c_i}^*) + \dot{x}_{rel}^*(t_{c_i}^*)\delta t_{c_i}$, the p_i nonlinear constraints can be linearized about the reference relative state vector $x_{rel}^*(t_{c_i}^*)$

$$\Psi_i\left[x_{rel}^*(t_{c_i}^*)\right] + \Psi_{x_{rel},i}\left[\delta x_{rel}(t_{c_i}^*) + \dot{x}_{rel}^*(t_{c_i}^*)\delta t_{c_i}\right], \quad i = 1, 2, \cdots, r \tag{118}$$

where

$$\Psi_{x_{rel},i} = \left.\frac{\partial \Psi}{\partial x_{rel}}\right|_{x_{rel}^*(t_{c_i}^*)}$$

In terms of the absolute states, the linearized constraint equations in Eq. 118 become

$$0 = \Psi_{x_{rel},i}M_{rel}\left[\delta x(t_{c_i}^*) + \dot{x}^*(t_{c_i}^*)\delta t_{c_i}\right] \tag{119}$$

where

$$\dot{x}^*(t^*_{c_i}) = \begin{bmatrix} \dot{x}_1(t^*_{c_i}) \\ \dot{x}_2(t^*_{c_i}) \end{bmatrix}$$

Substituting $\delta t_{c_i} = \mathsf{P}^{\delta t_{c_i}}_{\delta u}\delta u$ produces

$$\boxed{0 = \Psi_{x_{rel},i} M_{rel}\left[\delta x(t^*_{c_i}) + \dot{x}^*(t^*_{c_i})\mathsf{P}^{\delta t_{c_i}}_{\delta u}\delta u\right]} \tag{120}$$

where $\mathsf{P}^{\delta t_{c_i}}_{\delta u}$ represents the partial derivative of δt_{c_i} with respect to the targeting parameter vector δu.

Next, the dual-inertial state dispersion $\delta x(t^*_{c_i}) = [\delta x_1(t^*_{c_i}), \delta x_2(t^*_{c_i})]$ at time $t^*_{c_i}$ needs to be determined. The generic form for the active vehicle dispersion $\delta x_1(t^*_{c_i})$, whether for impulsive maneuvers or finite-burn maneuvers, is given by

$$\delta x_1(t^*_{c_i}) = M^1_{x_{c_i}x_0}\delta x_1(t^*_0) + M^1_{x_{c_i}\delta u}\delta u \tag{121}$$

where the targeting parameters δu and the matrices $M^1_{x_{c_i}x_0}$ and $M^1_{x_{c_i}\delta u}$ are dependent on the particular targeting problem (e.g., see Eqs. 16, 24, 31, and 67).

The coasting-flight dynamics model for passive Vehicle 2 is given in Eq. 9 where the passive vehicle dispersion, $\delta x_2(t^*_{c_i})$ is given simply by

$$\delta x_2(t^*_{c_i}) = \Phi(t^*_{c_i}, t^*_0)\delta x_2(t^*_0) = M^2_{x_{c_i}x_0}\delta x_2(t^*_0) \tag{122}$$

The dual-inertial state dispersion $\delta x(t^*_{c_i})$ is determined by combining Eqs. 121 and 122

$$\boxed{\delta x(t^*_{c_i}) = M_{x_{c_i}x_0}\delta x(t^*_0) + M_{x_{c_i}\delta u}\delta u} \tag{123}$$

where

$$M_{x_{c_i}x_0} = \begin{bmatrix} M^1_{x_{c_i}x_0} & 0 \\ 0 & M^2_{x_{c_i}x_0} \end{bmatrix}, \qquad M_{x_{c_i}\delta u} = \begin{bmatrix} M^1_{x_{c_i}\delta u} \\ 0 \end{bmatrix}$$

Substituting Eq. 123 into 120, produces

$$\boxed{0 = \Psi_{x_{rel},i} M_{rel}\left[M_{x_{c_i}x_0}\delta x(t^*_0) + \left\{M_{x_{c_i}\delta u} + \dot{x}^*(t^*_{c_i})\mathsf{P}^{\delta t_{c_i}}_{\delta u}\right\}\delta u\right]}$$

The equation above represents m constraint equations in n targeting parameters and can be written in the standard form

$$\boxed{\mathcal{M}\delta u = \mathcal{N}\delta x(t^*_0)} \tag{124}$$

where

$$\mathcal{M} = \begin{bmatrix} \Psi_{x_{rel},1} M_{rel}\left\{M_{x_{c_1}\delta u} + \dot{x}^*(t^*_{c_1})\mathsf{P}_{\delta t_{c_1},\delta u}\right\} \\ \Psi_{x_{rel},2} M_{rel}\left\{M_{x_{c_2}\delta u} + \dot{x}^*(t^*_{c_2})\mathsf{P}_{\delta t_{c_2},\delta u}\right\} \\ \vdots \\ \Psi_{x_{rel},r} M_{rel}\left\{M_{x_{c_r}\delta u} + \dot{x}^*(t^*_{c_r})\mathsf{P}_{\delta t_{c_r},\delta u}\right\} \end{bmatrix} \tag{125}$$

$$\mathcal{N} = -\begin{bmatrix} \Psi_{x_{rel},1} M_{rel} M_{x_{c_1}x_0} \\ \Psi_{x_{rel},2} M_{rel} M_{x_{c_2}x_0} \\ \vdots \\ \Psi_{x_{rel},r} M_{rel} M_{x_{c_r}x_0} \end{bmatrix} \tag{126}$$

8 CISLUNAR APPLICATIONS WITH GENERALIZED REFERENCE TARGETING

8.1 Cislunar Example 1: GRT Using Impulsive Burns

The main purpose of this first example is to show how generalized reference targeting and the generalized augmented state covariance (GAUSCOV) [11] analysis techniques can be used to plan impulsive maneuver control states ahead of their execution, and to show how the duration of the planning phase affects Δv dispersion and final position/velocity constraint dispersion. The targeting algorithm is based on the accompanied Generalized Reference Targeting document, Section 4. The targeting constraints (2) are the magnitudes of the final position and velocity vectors on a hyperbolic escape trajectory originating from low lunar orbit (LLO). For navigation, a Kalman filter provides lunar centered inertial (LCI) position vector measurements corrupted with noise (e.g., optical measurements of the earth, moon, or lunar surface features). For simplicity, two-body dynamics are assumed, and there are no actuator or sensor biases, scale-factors, and misalignment. The true state x and the navigation state $\hat{x}$ consist of the LCI position and velocity vectors. The control state consists of 1 impulsive maneuver at fixed time and a variable time for the final constraint $\hat{u} = [\Delta V_1, t_c]$. The GRT is used to plan a correction $\delta\hat{u} = [\delta V_1, \delta t_c]$ to the nominal maneuver and the final constraint time ΔT_p minutes before the nominal maneuver execution time.

The GAUSCOV propagation, update, and correction equations presented above are implemented using the problem parameters in Table 1 below. Several cases are investigated. The first case uses only the three targeting parameters of the maneuver impulse correction δV to achieve the final constraints. Figure 3 shows the 3-σ dispersion of position and velocity magnitude as a function of time with zero navigation errors. The targeting algorithm is executed 30 minutes prior to the impulsive maneuver, and the impulsive maneuver correction δV is computed and saved. Since the position and velocity have zero navigation error and the process noise is very small, the targeting solution is accurate, and the final dispersions are nearly zero. The required corrections to the x and y components of the impulse are (19.7, 22.7 m/s, 3-σ) are on the order of 2% of the nominal thrust, while the z component is much smaller.

Parameters	Values
Initial orbit	Low lunar orbit, circular, 100 km altitude
Initial mass	m_0^*=1000 kg
Final constraints	$\|r_f\|$ =2860 km, $\|v_f\|$ =2247 m/s, at t_c^* =3600 sec
Nominal Impulsive Maneuver	Δv=[-795.3 m/s -606.2 m/s -0.4 m/s], at t_m^* =2500 sec
Initial state dispersion	σ_{r_0} =3.33 km, σ_{v_0}=3.33 m/s
Planning phase duration	ΔT_p =30 min, 10 min
True/filter model sensor noise	$\sigma_\nu = \hat{\sigma}_\nu$ =0 m, 1000 m
True/filter model process noise	$\sigma_\omega = \hat{\sigma}_\omega$ =1.0e-8 m/s
True/filter model actuator noise	$\sigma_\xi = \hat{\sigma}_\xi$ = 0 N

Table 1. Parameters for Example 2 and Example 3

Figure 4 shows the 3-σ dispersion of position and velocity magnitude as a function of time with navigation errors on. On the left, the targeting algorithm is executed 30 minutes prior maneuver execution, and the impulse correction δV is computed and saved. However, because the navigation errors are large at that time (not shown in the figure), the targeting solution is inaccurate and results in large final dispersions. On the right, the targeting algorithm is executed only 10 minutes before maneuver execution when the navigation errors are much smaller. The results in a more accurate targeting solution and near zero final dispersion (compare to the case with zero navigation errors above).

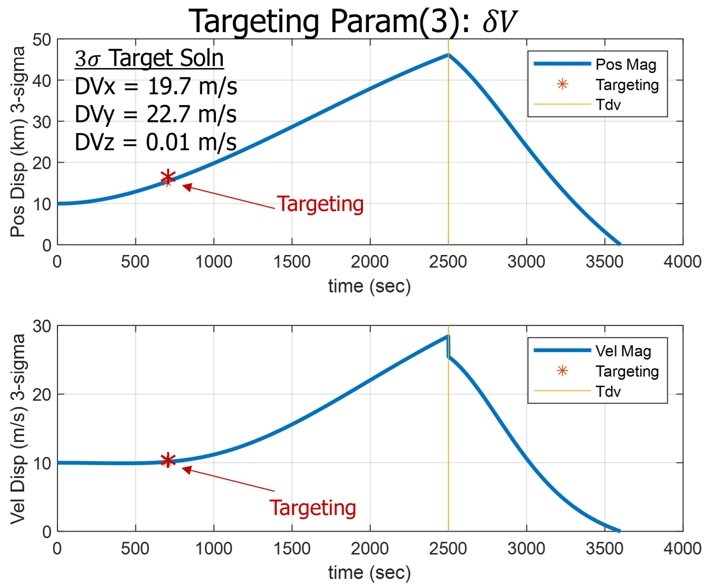

Figure 3. 3-σ dispersion of position and velocity magnitude as a function of time with zero navigation errors. The targeting algorithm computes and plans the required correction to the maneuver impulse δV, 30 minutes prior to the maneuver execution.

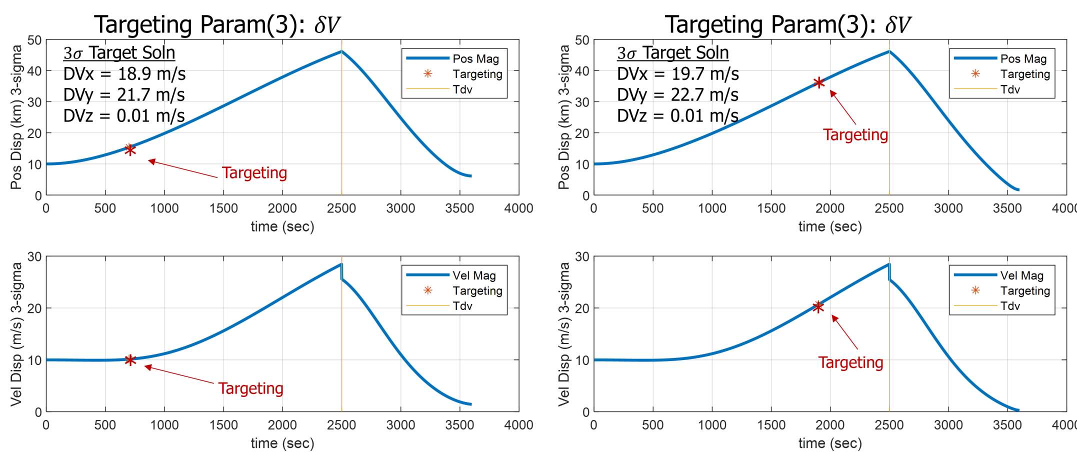

Figure 4. 3-σ dispersion of position and velocity magnitude as a function of time with navigation errors on. The targeting algorithm computes and plans the required correction to the maneuver impulse δV, 30 minutes prior to maneuver execution (left) or 10 minutes prior to the maneuver execution (right).

The second case uses four targeting parameters δV and δt_f to achieve the final constraints. Figure 5 shows the 3-σ dispersion of position and velocity magnitude as a function of time with zero navigation errors. The targeting algorithm is executed 30 minutes prior engine ignition, and the targeting solution, δV and δt_f, are computed and saved. Since the position and velocity have zero navigation error and the process noise is very small, the targeting solution is accurate, and the final dispersions are nearly zero. Notice also that the required corrections to the x and y components of the maneuver impulse (5.4, 3.7 m/s, 3-σ) have been reduced by an order of magnitude by introducing the additional targeting parameter δt_f. The 3-σ value for the additional targeting parameter 10.8 seconds.

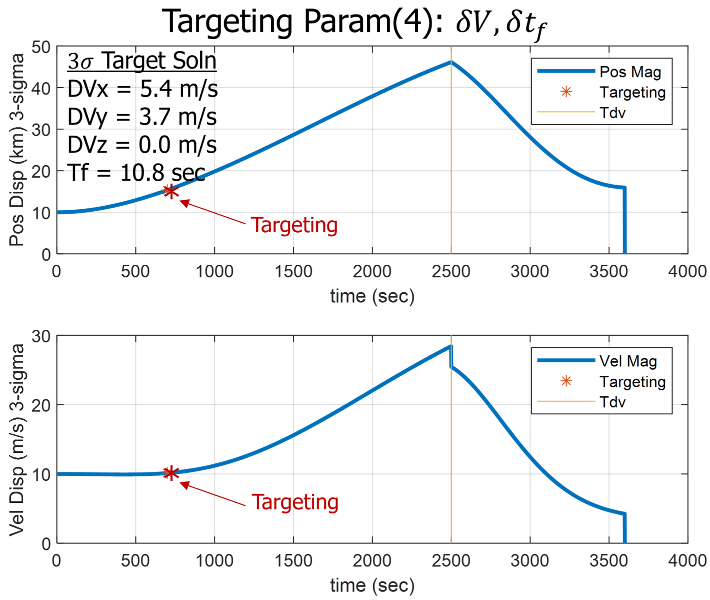

Figure 5. 3-σ dispersion of position and velocity magnitude as a function of time with zero navigation errors. The targeting algorithm computes and plans the required correction to the maneuver impulse δV and final constraint time δt_f, 30 minutes prior to the maneuver execution.

Figure 6 shows the 3-σ dispersion of position and velocity magnitude as a function of time with navigation errors on. On the left, the targeting algorithm is executed 30 minutes prior to maneuver execution, and the four targeting parameters δV and δt_f are computed and saved. However, because the navigation errors are large at that time (not shown in the figure), the targeting solution is inaccurate and results in large final dispersion. On the right, the targeting algorithm is executed only 10 minutes before engine ignition when the navigation errors are much smaller. This results in a more accurate targeting solution (compare to the case with zero navigation errors above).

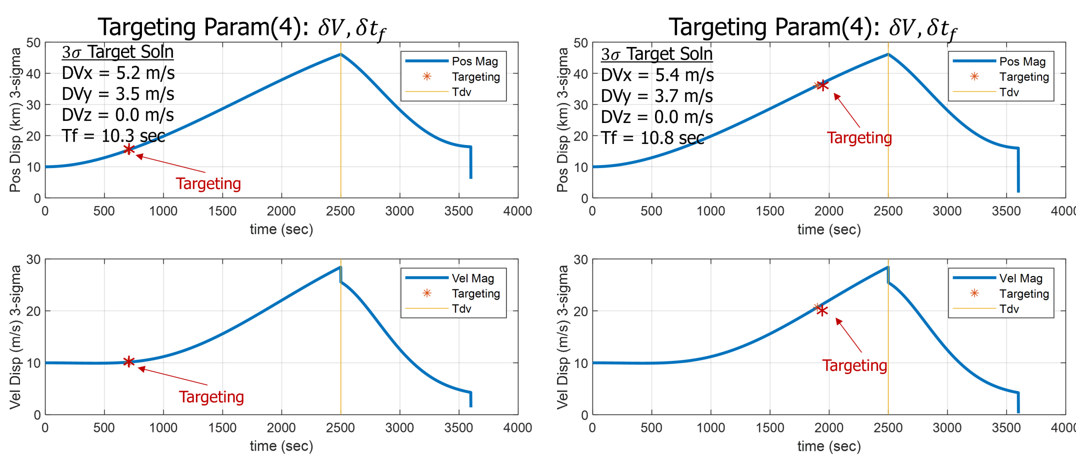

Figure 6. 3-σ dispersion of position and velocity magnitude as a function of time with navigation errors on. The targeting algorithm computes and plans the required correction to the maneuver impulse δV and final constraint time δt_f, 30 minutes prior to the maneuver execution (left) or 10 minutes prior to the maneuver execution (right).

8.2 Cislunar Example 2 - GRT Using Finite Burns with Varying Thrust Vector

The main purpose of Example 2 is to show how a GAUSCOV analysis tool can be used to plan finite-burn control states ahead of their execution, and to show how the duration of the planning phase affects Δv dispersion and final position/velocity constraint dispersion. The targeting algorithm is based on the accompanied GRT formulation using finite burns with the thrust vector outlined in Section 5. The two targeting constraints are the magnitudes of the final position and velocity vectors on a hyperbolic escape trajectory originating from low lunar orbit. The nominal trajectory consists of an initial coasting-flight phase, followed by a powered-flight phase, with a final coasting flight phase as shown in Figure 7. For navigation, a Kalman

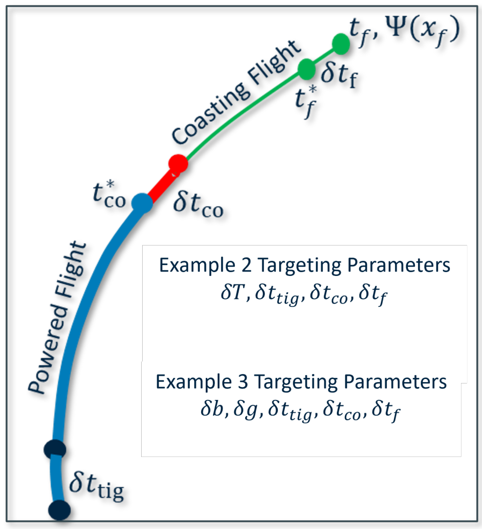

Figure 7. Nominal trajectory with variable time of engine ignition, variable time of engine cutoff, and variable final constraint time.

filter provides inertial LCI position vector measurements corrupted with noise (e.g., optical measurements of the earth, moon, or lunar surface features). For simplicity, two-body dynamics are assumed, and there are no actuator or sensor biases, scale-factors, and misalignment. The true state x and the navigation state $\hat{x}$ consist of the LCI position and velocity vectors r , v, the mass of the vehicle m, and thrust efficiency α=constant (defined as one divided by the engine exhaust velocity). The control state consists of the thrust vector, the time of engine ignition, the time of engine cutoff, and a variable time for the final constraint $\hat{u} = [T, t_{tig}, t_{co}, t_c]$. The GRT is used to plan a set of constant control state corrections $\delta\hat{u} = [\delta T, \delta t_{tig}, \delta t_{co}, \delta t_c]$. It is assumed this targeting algorithm is executed is ΔT_p minutes before the nominal maneuver execution time.

The GAUSCOV propagation, update, and correction equations presented above are implemented using the problem parameters in Table 2. Several cases are investigated. The first case uses only three targeting parameters δT to achieve the final constraints. Figure 8 shows the 3-σ dispersion of position and velocity magnitude as a function of time with zero navigation errors. The targeting algorithm is executed 30 minutes prior engine ignition, and the thrust vector perturbation δT is computed and saved. Since the position and velocity have zero navigation error and the process noise is very small, the targeting solution is accurate, and the final dispersions are nearly zero. The required perturbations to the x and y components of the thrust vector (16.0, 20.6 N, 3-σ) are on the order of 2% of the nominal thrust, while the z component is much smaller.

Parameters	Values
Initial orbit	Low lunar orbit, circular, 100 km altitude
Initial mass, thrust, and Isp	m_0^*=1000 kg, T^*=981 N, α^*=400 sec
Final constraints	$\|r_f\|$ =3022 km, $\|v_f\|$ =2324 m/s, at t_c^* =3600 sec
Nominal powered-flight time	t_{tig}^* =2000 sec, t_{co}^* =3000 sec
Initial state dispersion	σ_{r_0} =3.33 km, σ_{v_0}=3.33 m/s, σ_{m_0} =0 kg, σ_{α_0} =0 s/m
Planning phase duration	ΔT_p =30 min, 10 min
True/filter model sensor noise	$\sigma_\nu = \hat{\sigma}_\nu$ =0.0 m, 333.0 m
True/filter model process noise	$\sigma_\omega = \hat{\sigma}_\omega$ =1.0e-8 m/s
True/filter model actuator noise	$\sigma_\xi = \hat{\sigma}_\xi$ =0.0 N

Table 2. Parameters for Example 2 and Example 3

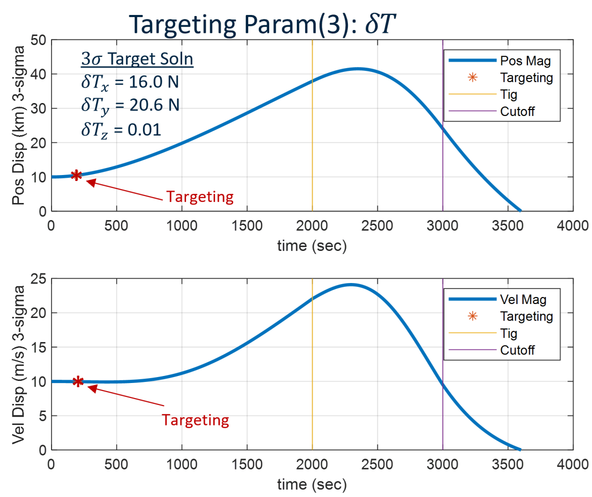

Figure 8. 3-σ dispersion of position and velocity magnitude as a function of time with zero navigation errors. The targeting algorithm computes and plans the required perturbation to thrust vector δT, 30 minutes prior to the start of powered-flight.

Figure 9 shows the 3-σ dispersion of position and velocity magnitude as a function of time with navigation errors on. On the left, the targeting algorithm is executed 30 minutes prior engine ignition, and the thrust vector perturbation δT is computed and saved. However, because the navigation errors are large at that time (not shown in the figure), the targeting solution is inaccurate and results in large final dispersions. On the right, the targeting algorithm is executed only 10 minutes before engine ignition when the navigation errors are much smaller. This results in a more accurate targeting solution and near zero final dispersion (compare to the case with zero navigation errors above).

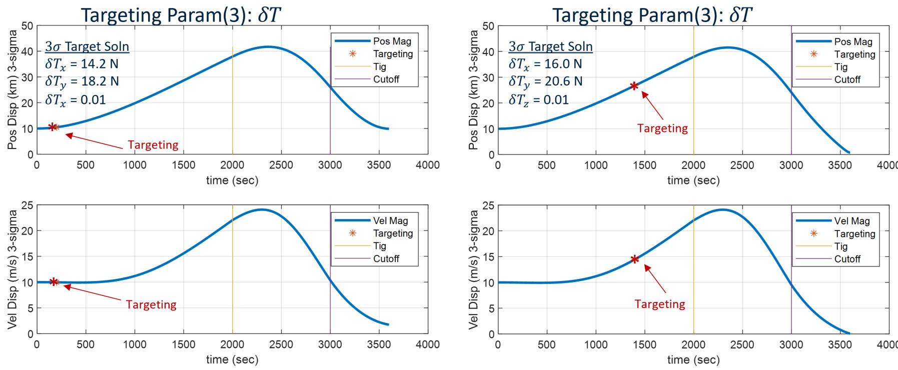

Figure 9. 3-σ dispersion of position and velocity magnitude as a function of time with navigation errors on. The targeting algorithm computes and plans the required perturbation to thrust vector δT, 30 minutes prior to the start of powered-flight (left) or 10 minutes prior to the start of powered-flight (right).

The second case uses six targeting parameters δT, δt_{tig}, δt_{co}, and δt_f to achieve the final constraints. Figure 10 shows the 3-σ dispersion of position and velocity magnitude as a function of time with zero navigation errors. The targeting algorithm is executed 30 minutes prior engine ignition, and the targeting solutions, δT, δt_{tig}, δt_{co}, and δt_f, are computed and saved. Since the position and velocity have zero navigation error and the process noise is very small, the targeting solution is accurate, and the final dispersions are nearly zero. Notice also that the required perturbations to the x and y components of the thrust vector (2.3, 2.8 N, 3-σ) have been reduced by an order of magnitude by introducing the additional targeting parameters, δt_{tig}, δt_{co}, and δt_f. The 3-σ values for the three additional targeting parameters are only 7.5 seconds or smaller.

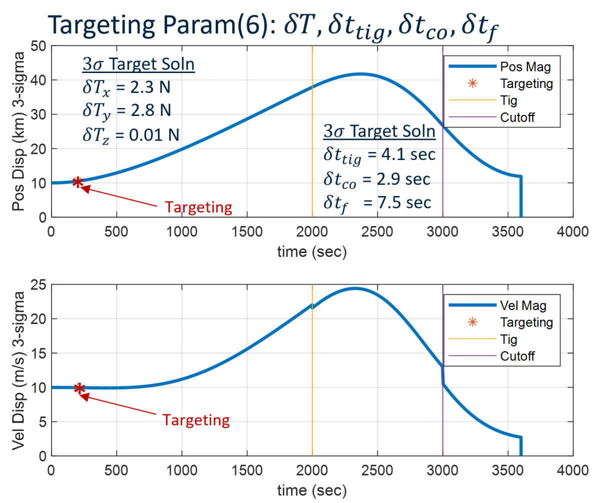

Figure 10. 3-σ dispersion of position and velocity magnitude as a function of time with zero navigation errors. The targeting algorithm computes and plans the required perturbations to thrust vector δT, ignition time δt_{tig}, cutoff time δt_{co}, and final constraint time δt_f, 30 minutes prior to the start of powered-flight.

Figure 11 shows the 3-σ dispersion of position and velocity magnitude as a function of time with navigation errors on. On the left, the targeting algorithm is executed 30 minutes prior engine ignition, and the six targeting parameters δT, δt_{tig}, δt_{co}, and δt_f are computed and saved. However, because the navigation errors are large at that time (not shown in the figure), the targeting solution is inaccurate and results in large final dispersion. On the right, the targeting algorithm is executed only 10 minutes before engine ignition when the navigation errors are much smaller. This results in a more accurate targeting solution and near zero final dispersion (compare to the case with zero navigation errors above).

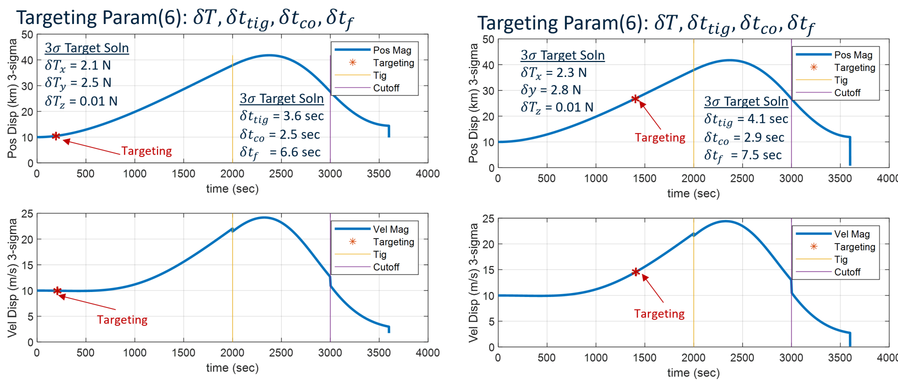

Figure 11. 3-σ dispersion of position and velocity magnitude as a function of time with navigation errors on. The targeting algorithm computes and plans the required perturbations to thrust vector δT, ignition time δt_{tig}, cutoff time δt_{co}, and final constraint time δt_f, 30 minutes prior to the start of powered-flight (left) or 10 minutes prior to the start of powered-flight (right).

8.3 Cislunar Example 3 - GRT Using Finite Burns with Fixed Thrust Magnitude

This section presents another example of incorporating finite-burn targeting into a GAUSCOV analysis tool. The key difference in this example is the control states. Instead of a perturbation to the nominal thrust vector δT, the control state in this section includes a perturbation to the initial thrust direction δb and a perturbation to the thrust turning rate δg, i.e., the control states are $\delta p = [\delta b, \delta g, \delta t_{tig}, \delta t_{co}, \delta t_f]$ instead of $\delta p = [\delta T, \delta t_{tig}, \delta t_{co}, \delta t_f]$. All other elements of this example remain the same as in Example 2 including the values of the problem parameters in Table 2. The targeting algorithm used to determine the new control state are documented in the accompanied Section 6.

Several cases are investigated. The first case uses only four targeting parameters, δb and δg, to achieve the final constraints. Figure 12 shows the 3-σ dispersion of position and velocity magnitude as a function of time with zero navigation errors. The targeting algorithm is executed 30 minutes prior engine ignition, and the initial thrust direction δb and turning rate δg are computed and saved. Since the position and velocity have zero navigation error and the process noise is very small, the targeting solution is accurate, and the final dispersions are nearly zero. The 3-σ magnitudes of the required perturbations δb and δg are 8.7 deg and 0.23 deg/s, respectively. The perturbation to the thrust turning rate is much too high and unrealistic.

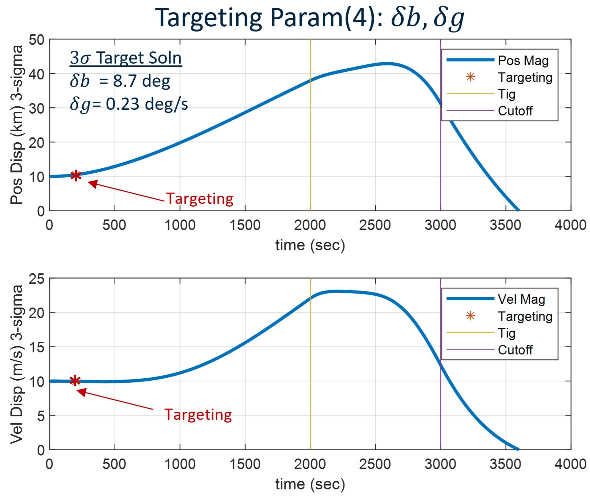

Figure 12. 3-σ dispersion of position and velocity magnitude as a function of time with zero navigation errors. The targeting algorithm computes and plans the required perturbations to the initial thrust direction δb and turning rate δg, 30 minutes prior to the start of powered-flight.

Figure 13 shows the 3-σ dispersion of position and velocity magnitude as a function of time with navigation errors on. On the left, the targeting algorithm is executed 30 minutes prior engine ignition, and δb and δg are computed and saved. However, because the navigation errors are large at that time (not shown in the figure), the targeting solution is inaccurate and results in large final dispersion. On the right, the targeting algorithm is executed only 10 minutes before engine ignition when the navigation errors are much smaller. This results in a more accurate targeting solution and near zero final dispersion (compare to the case with zero navigation errors above). The perturbation to the thrust turning rate is still unrealistic.

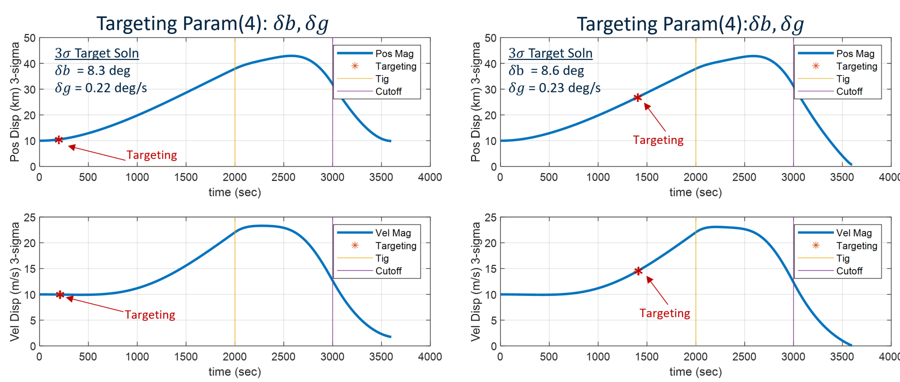

Figure 13. 3-σ dispersion of position and velocity magnitude as a function of time with navigation errors on. The targeting algorithm computes and plans the required perturbations to the initial thrust direction δb and turning rate δg, 30 minutes prior to the start of powered-flight (left) or 10 minutes prior to the start of powered-flight (right).

The second case uses seven targeting parameters δb, δg, δt_{tig}, δt_{co}, and δt_f to achieve the final constraints. Figure 14 shows the 3-σ dispersion of position and velocity magnitude as a function of time assuming zero navigation errors. The targeting algorithm is executed 30 minutes prior engine ignition, and all seven targeting parameters, δb, δg, δt_{tig}, δt_{co}, and δt_f, are computed and saved. Since the position and velocity have zero navigation error and the process noise is very small, the targeting solution is accurate, and the final dispersions are nearly zero. By adding the three additional targeting parameters, δt_{tig}, δt_{co}, and δt_f, the 3-σ magnitudes of δb and δg are reduced to only 0.0003 deg and 0.0.005 deg/s, respectively, and the 3-σ values of δt_{tig}, δt_{co}, and δt_f, are less than 1.7 seconds.

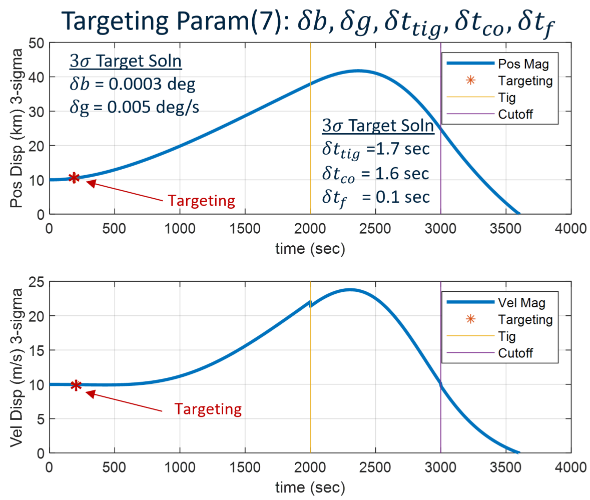

Figure 14. 3-σ dispersion of position and velocity magnitude as a function of time with zero navigation errors. The targeting algorithm computes and plans the required perturbations to the initial thrust direction δb, turning rate δg, ignition time δt_{tig}, cutoff time δt_{co}, and final constraint time δt_f, 30 minutes prior to the start of powered-flight.

Figure 15 shows the 3-σ dispersion of position and velocity magnitude as a function of time with navigation errors on. On the left, the targeting algorithm is executed 30 minutes prior engine ignition, and the seven targeting parameters are computed and saved. However, because the navigation errors are large at that time (not shown in the figure), the targeting solution is inaccurate and results in large final dispersions. On the right, the targeting algorithm is executed only 10 minutes before engine ignition when the navigation errors are much smaller. This results in a more accurate targeting solution and near zero final dispersions (compare to the case with zero navigation errors above).

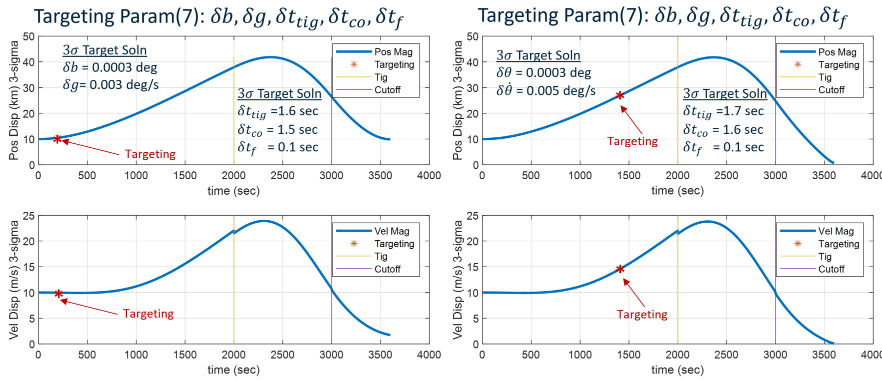

Figure 15. 3-σ dispersion of position and velocity magnitude as a function of time with navigation errors on. The targeting algorithm computes and plans the required perturbations to the initial thrust direction δb, turning rate δg, ignition time δt_{tig}, cutoff time δt_{co}, and final constraint time δt_f, 30 minutes prior to the start of powered-flight (left) or 10 minutes prior to the start of powered-flight (right).

9 CONCLUSIONS

This paper outlined a generalized reference targeting (GRT) algorithm that accommodates arbitrary flight dynamics, both impulsive and finite burns, and either absolute or relative targeting applications. It also allows for an arbitrary number of targeting design parameters such as multiple discrete correction burns or finite thrust parameters to satisfy numerous combinations of targeting constraints that can have fixed or variable time epochs. Given a reference trajectory, this targeting technique provides a general framework to quickly solve an assortment of targeting problems that may be well-defined, over-determined, or under-determined while naturally producing metrics providing insight into the controllability for a given problem formulation. Due to the derivation, speed, and accuracy of the algorithm, it lends to supporting rapid linear covariance analysis and robust trajectory design applications for a variety of flight phases such as rendezvous and docking, cislunar transfer, interplanetary flight, orbit maintenance, de-orbit, and powered descent and landing.

REFERENCES

[1] G. Gómez, J. Masdemont, and C. Simó, “Quasihalo orbits associated with libration points,” *The Journal of the Astronautical Sciences*, Vol. 46, 1998, pp. 135–176.

[2] D. J. Grebow, M. T. Ozimek, and K. C. Howell, “Advanced modeling of optimal low-thrust lunar pole-sitter trajectories,” *Acta Astronautica*, Vol. 67, No. 7-8, 2010, pp. 991–1001.

[3] K. Howell, D. Grebow, and Z. Olikara, “Design using Gauss perturbing equations with applications to lunar south pole coverage,” *Adv. Astronaut. Sci*, Vol. 127, 2007, pp. 641–670.

[4] S. Scarritt, B. Marchand, A. J. Brown, W. H. Tracy, and M. W. Weeks, “Finite-burn linear targeting algorithm for autonomous path planning and guidance,” *Journal of Guidance, Control, and Dynamics*, Vol. 35, No. 5, 2012, pp. 1605–1615.

[5] S. K. Scarritt, T. Fill, and S. Robinson, “Advances in Orion’s On-Orbit Guidance and Targeting System Architecture,” *AAS Guidance Navigation and Control Conference*, No. JSC-CN-32859, 2015.

[6] C. E. York and K. C. Howell, “A two-level differential corrections algorithm for low-thrust spacecraft trajectory targeting,” *29th AAS/AIAA Space Flight Mechanics Meeting*, 2019, pp. 1–20.

[7] H. B. Keller, *Numerical solution of two point boundary value problems*. SIAM, 1976.

[8] J. Stoer, R. Bulirsch, R. Bartels, W. Gautschi, and C. Witzgall, *Introduction to numerical analysis*, Vol. 1993. Springer, 1980.

[9] T. A. Lovell and D. A. Spencer, “Relative orbital elements formulation based upon the Clohessy-Wiltshire equations,” *The Journal of the Astronautical Sciences*, Vol. 61, 2014, pp. 341–366.

[10] R. H. Battin, *An introduction to the mathematics and methods of astrodynamics*. Aiaa, 1999.

[11] D. K. Geller, C. York, and D. Woffinden, “Generalized Augmented-State Covariance Analysis for Spaceflight,” *AAS 25-065, AAS Guidance and Control Conference, Breckenridge, CO, February 2025*, 2025.